EFFECT OF PLANE STRAIN ON PORE PRESSURE PARAMETERS

by

HARI KRISHAN MITTAL

B.A.Sc., UNIVERSITY OF BRITISH COLUMBIA, 1961

A THESIS SUBMITTED IN PARTIAL FULFILMENT OF
THE REQUIREMENTS FOR THE DEGREE OF
M.A.Sc.

IN THE DEPARTMENT
OF
CIVIL ENGINEERING

We accept this thesis as conforming to the
required standard

THE UNIVERSITY OF BRITISH COLUMBIA

April, 1963

In presenting this thesis in partial fulfilment of the requirements for an advanced degree at the University of British Columbia, I agree that the Library shall make it freely available for reference and study. I further agree that permission for extensive copying of this thesis for scholarly purposes may be granted by the Head of my Department or by his representatives. It is understood that copying or publication of this thesis for financial gain shall not be allowed without my written permission.

Department of Civil Engineering

The University of British Columbia,
Vancouver 8, Canada.

Date May 8, 1963

ABSTRACT

A theoretical as well as a laboratory investigation into the effects of plane strain on pore pressure parameters is presented. Other observations relative to stress-strain relationships, intermediate principal stress values and shear strength parameters (c', ϕ') in terms of effective stresses are also reported.

Experimental work consisted of the following three types of Undrained Triaxial tests with pore pressure measurements:

(1) Standard triaxial tests on cylindrical specimens.

(2) Triaxial tests on rectangular specimens.

(3) Confined tests on rectangular specimens, in which lateral expansion was prevented in one direction, to achieve plane strain condition.

A strain-controlled triaxial machine equipped with a non-flow null indicating type pore pressure measuring device was used for all shear tests.

The observed data show that for the soil tested the values of pore pressure parameter A_f and shear strength parameter (c', ϕ') under plane strain condition are higher than those obtained in corresponding triaxial tests. Failure is observed to occur, in the case of plane strain tests, at strains much smaller than those for the corresponding triaxial tests.

ACKNOWLEDGMENT

The author wishes to express his appreciation and indebtedness to his supervisor, Mr. N.D. Nathan, for assistance in all stages of this undertaking. He also wishes to thank the staff, of the Department of Civil Engineering Workshop, for the help rendered in designing and Constructing the equipment required for the experimental work of this thesis.

CONTENTS

ILLUSTRATIONS

LIST OF TABLES

NOTATIONS

A_f	Pore Pressure Parameter: axial
a	Area
a_o	Initial Area of Specimens
B	Pore Pressure Parameter: all round
c	Apparent Cohesion: effective stresses
C_c	Compressibility of soil skeleton
C_w	Compressibility of water
e	Void ratio
e_{a_o}	Initial void ratio
E	Young's modulus of elasticity
h or H	Co-efficient of air solubility in water by volume
M_{50}	Secant Modulus of deformation: 50% of maximum deviator stress
N	Porosity
p	For plane strain: suffix
Pa	initial air pressure
S	Degree of saturation
T	For triaxial test: suffix
U	Pore pressure
U_o	Pore pressure: all round
Ua	Pore air pressure
U_c	Pore pressure differential: capillary
U_w	Pore water pressure
V	Volume
CT	Cylindrical triaxial tests
PS	Plane strain tests
RT	Rectangular triaxial tests

α_f	Angle of failure plane to major principal plane
γ_d	Dry density
ϵ	Unit axial strain
Δ	Incremental change: prefix
μ	Poisson's ratio
σ_t	Total stress
$\bar{\sigma}$	Effective stress
$\bar{\sigma}_f$	Effective stress normal to the failure plane
σ_1	Major principal stress: total
$\bar{\sigma}_1$	Major principal stress: effective
σ_2	Intermediate principal stress: total
$\bar{\sigma}_2$	Intermediate principal stress: effective
σ_3	Minor principal stress: total
$\bar{\sigma}_3$	Minor principal stress: effective
τ_f	Shear stress on the failure plane

I. INTRODUCTION

As the number and size of embankments, earthdams, and other earth structures being designed and constructed increase, the study of strength characteristics of compacted cohesive soils is gaining importance. For satisfactory and economical design, a knowledge of the behaviour of compacted cohesive soils under load is essential; for the laboratory measurements of shear strength under controlled conditions of drainage, and of deformation characteristics (other than compressibility) the civil engineer is usually dependent on the triaxial test.

It may be noted that many practical problems approximate more closely to conditions of plane strain than to the axial symmetry obtained in the conventional triaxial test.

It appears that the strength characteristics corresponding to plane strain are somewhat different from those obtained by the standard triaxial test. There is little direct evidence of the magnitude of this difference, which is only one of several factors influencing the relationship between laboratory measurements and the actual field values of the shear characteristics of compacted clays.

However, the author has made a pilot investigation to determine the effect of plane strain on pore pressure and strength in undrained shear. Owing to the limited amount of reliable test data so far available, only tentative conclusions can be drawn at this stage.

II. THEORETICAL CONSIDERATIONS

A. Effective stress in Soils

The stresses which govern the shear strength and changes in volume of a soil skeleton are defined as the "Effective Stresses", $\bar{\sigma}$. For saturated soils in which the pore spaces are filled with water, it was shown experimentally by Terzaghi (1923) that:

$$\bar{\sigma} = \sigma_t - U_w \quad \ldots\ldots\ldots\ldots\ldots\ldots (1)$$

where σ_t denotes the total normal stress and U_w denotes the water pressure in the void space.

Thus for an equal all-round stress the relationship between the effective stress and the volume changes in the soil is given quantitatively by the expression:

$$\frac{\Delta V}{V} = -C_c\,(\bar{\sigma}) \quad \ldots\ldots\ldots\ldots\ldots\ldots (2)$$

where $\frac{\Delta V}{V}$ = the volume change per unit volume of soil

C_c = the compressibility of the soil skeleton (Here used with respect to isotropic compression.)

and in terms of the modified coulomb criterion the shearing strength, denoted by τ_f , is given by the expression:

$$\tau_f = c' + \bar{\sigma}_f \operatorname{Tan} \phi' \quad \ldots\ldots\ldots (3)$$

where c' = the apparent cohesion) in terms of

ϕ' = the angle of shearing resistance) effective stresses.

$\bar{\sigma}_f$ = the effective normal stress on the failure plane

In the case of partly saturated soils the void space contains both air and water which, due to surface tension, may be in equilibrium at widely different pressures. A more general form of expression for effective stress to account for this condition was put forward by Bishop (1955),

$$\bar{\sigma} = \sigma_t - \left(U_a - \chi\,(U_a - U_w)\right) \quad \ldots\ldots\ldots (4)$$

To follow page 2.

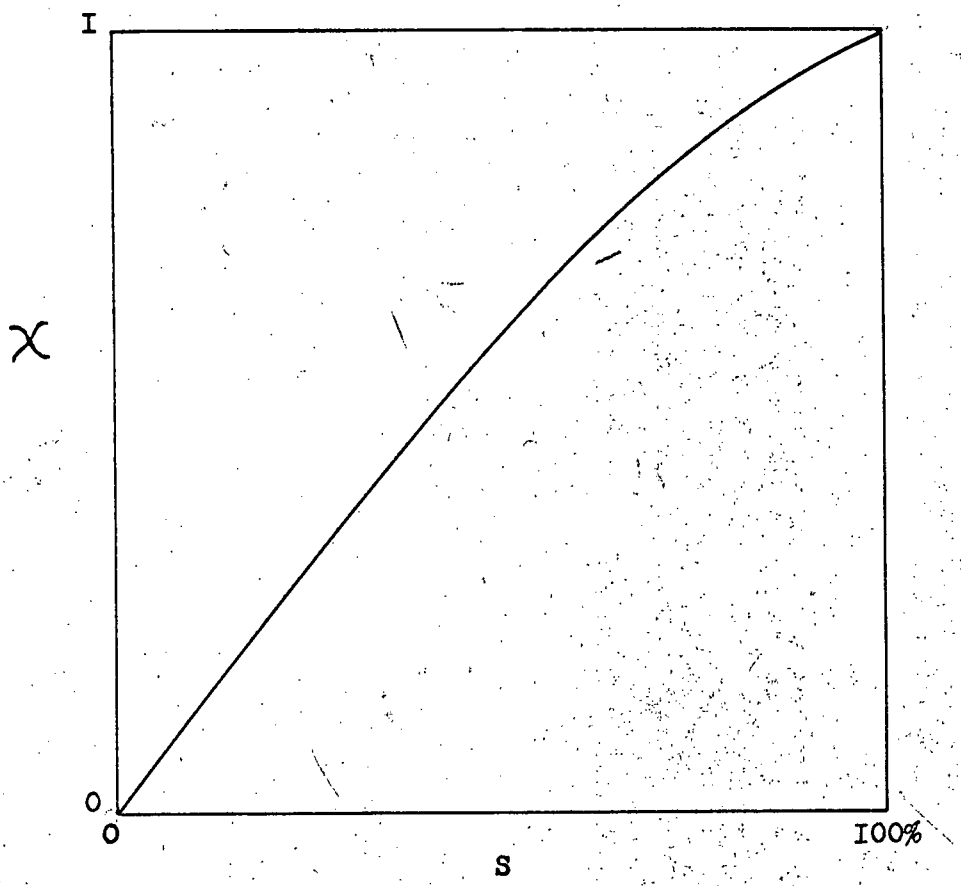

Figure - I. ANTICIPATED RELATIONSHIP BETWEEN THE PARAMETER χ AND THE DEGREE OF SATURATION S, BISHOP(1955).

where u_a denotes pressure of air in the pore space and χ is a parameter closely related to the degree of saturation, S, and varying from unity in saturated soils to zero in dry soils (Fig. 1).

However, the large positive pore pressures likely to lead to instability in rolled fills are only experienced at high degrees of saturation, where may be equated to unity with little error. The additional complication of observing or predicting pore air pressure is therefore hardly justified in such cases.

B. Prediction of Pore Pressures

In the design of fills, then it is necessary to be able to predict the pore pressures that will be developed at all points in the fill, when the total pressures only are known. Current methods of doing this will now be presented, and attention will be drawn to the significance of the strain conditions.

(i) Imperial College Method

For the idealized case in which the compressible skeleton of soil particles behaves as an elastic isotropic material and the fluid in the pore space shows a linear relationship between volume change and stress, Bishop and Henkel (1957) have shown that the pore pressure change, for the no drainage condition in a conventional triaxial test ($\sigma_2 = \sigma_3$), can be given by the equation:

$$= \frac{1}{1 + N(\frac{C_w}{C_c})} \left(\Delta\sigma_3 + \frac{1}{3} (\Delta\sigma_1 - \Delta\sigma_3) \right) \quad \ldots\ldots\ldots (5)$$

where C_c = $3 (1-2\mu)/E$, the compressibility of the soil skeleton

E = Young's modulus of elasticity

μ = Poisson's ratio with respect to changes in effective stress

$\Delta\sigma_1$ = change in major principal stress

$\Delta\sigma_3$ = change in minor principal stress

N = Initial porosity

C_w = Compressibility of the fluid in the pore space

In practice, however, it is recognised that the volume change characteristics of the soil skeleton are non-linear; but it is apparent from equation (5) that a change in pore pressure consists of two components:

(1) One due to the change in all-round pressure

(2) One due to the change in deviator stress

Thus the pore pressure changes are expressed in terms of two empirical parameters A and B (Skempton (1954)), where

$$\Delta U = B\{\Delta\sigma_3 + A(\Delta\sigma_1 - \Delta\sigma_3)\} \quad \ldots\ldots\ldots\ldots (6)$$

For fully saturated soils the value of C_w - the compressibility of pore fluid (water alone in this case) - is so small that the value of parameter B can be taken to be almost equal to unity. In the case of partly saturated soils, however, the value of C_w is much higher because the void space contains both water and air. The value of parameter B, for partly saturated soils, is, therefore, less than unity and varies with the stress range. The value of B which applies during the application of cell pressure ($\Delta\sigma_3$) is, thus, not equal to the value which is applicable for the duration of increase in deviator stress ($\Delta\sigma_1 - \Delta\sigma_3$). Hence it is wise not to separate the terms in the product B.A but to denote it by a single parameter A_f and express equation (6) in the form:

$$\Delta U = B\Delta\sigma_3 + A_f(\Delta\sigma_1 - \Delta\sigma_3) \quad \ldots\ldots\ldots\ldots (7)$$

Triaxial tests are performed to determine B and A_f, and field pore pressures are determined on the basis of parameters so found. The A_f and B values can be established for the $\frac{\sigma_1}{\sigma_3}$ ratio that is expected to apply in the field, but they can only be found for the case of $\sigma_2 = \sigma_3$ in the conventional test.

It should be noted that equation (7) is derived on the basis of axial symmetry ($\Delta\sigma_2 = \Delta\sigma_3$) and, thus, takes no account of the change in the intermediate principal stress ($\Delta\sigma_2$). In the majority of stability problems the condition approximate very closely to plane strain, in which the intermediate principal stress (σ_2) is not equal to the minor principal stress (σ_3) as in the case of the conventional triaxial test. The pore pressure change for the idealized elastic soil, under the plane strain condition $\left\{\Delta\bar{\sigma}_2 = \mu(\Delta\bar{\sigma}_3 + \Delta\bar{\sigma}_1)\right\}$, may be expressed as:

(1)
$$\Delta U = \frac{1}{1 + \bar{N}\left(\frac{C_w}{C_c}\right)}\left\{\Delta\sigma_3 + \frac{1}{2}(\Delta\sigma_1 - \Delta\sigma_3)\right\} \quad \ldots\ldots\ldots\ldots \quad (8)$$

where $C_c = 2(1 + \mu)(1 - 2\mu)/E$, which represents the volume change characteristics in plane strain under changes in σ_1 and σ_3.

It is clear from equation (6) that the basic form of expression for pore pressure change in plane strain is the same as in equation (7).

At this stage it may be interesting to study the effect of plane strain on the pore pressure parameters, B and A_f, as defined in equation (7), in the case of idealized elastic soil. From equations (5) and (8) the expressions

---

(1) For derivation of this equation see Bishop and Henkel (1957), p.8.

for pore pressure parameters are:

$$A_{f_T} = \frac{1}{3}\left(\frac{1}{1 + N\frac{C_w\,(E)}{3(1-2\mu)}}\right) \quad \ldots\ldots\ldots\ldots\ldots\ldots \quad (9)$$

$$A_{f_p} = \frac{1}{2}\left(\frac{1}{1 + N\frac{C_w\,(E)}{2(1+\mu)(1-2\mu)}}\right) \quad \ldots\ldots\ldots\ldots\ldots \quad (10)$$

and $$\frac{B_p}{B_T} = \frac{2}{3}\left(\frac{A_{f_p}}{A_{f_T}}\right) \quad \ldots\ldots\ldots\ldots\ldots\ldots\ldots\ldots \quad (11)$$

where A_{f_T} = Parametic A_f in equation (7) for triaxial test

A_{f_p} = Parametic A_f in equation (7) for plane strain

B_T = Parametic B in equation (7) for triaxial test

B_p = Parametic B in equation (7) for plane strain

From equation (9) it follows that

$$A_{f_T} = \frac{1}{3}\left(\frac{1}{1 + \alpha/3}\right) \quad \ldots\ldots\ldots\ldots\ldots\ldots\ldots \quad (12)$$

where $\alpha = N\frac{C_w\,(E)}{(1-2\mu)}$

Similarly from equation (10) we obtain the following expression

$$A_{f_p} = \frac{1}{2}\left(\frac{1}{1 + \frac{\alpha}{2(1+\mu)}}\right) \quad \ldots\ldots\ldots\ldots\ldots\ldots \quad (13)$$

By eliminating α from equations (12) and (13) we get

$$A_{f_p} = \frac{(1+\mu)\,A_{f_T}}{1 - (1-2\mu)A_{f_T}} \quad \ldots\ldots\ldots\ldots\ldots\ldots \quad (14)$$

For an ideal material, with Poisson's ratio of 0.5, this would reduce to $A_{f_p} = 1.5\,A_{f_T}$, and, from equation (11), it would follow that $B_p = B_T$. However, values of Poisson's ratio for clayey soils may be of the order of 0.45;(2)

---

(2) For Poisson's ratio of clayey soils see "Foundation Engineering" edited by G.A. Leonards, p. 789.

To follow page 6.

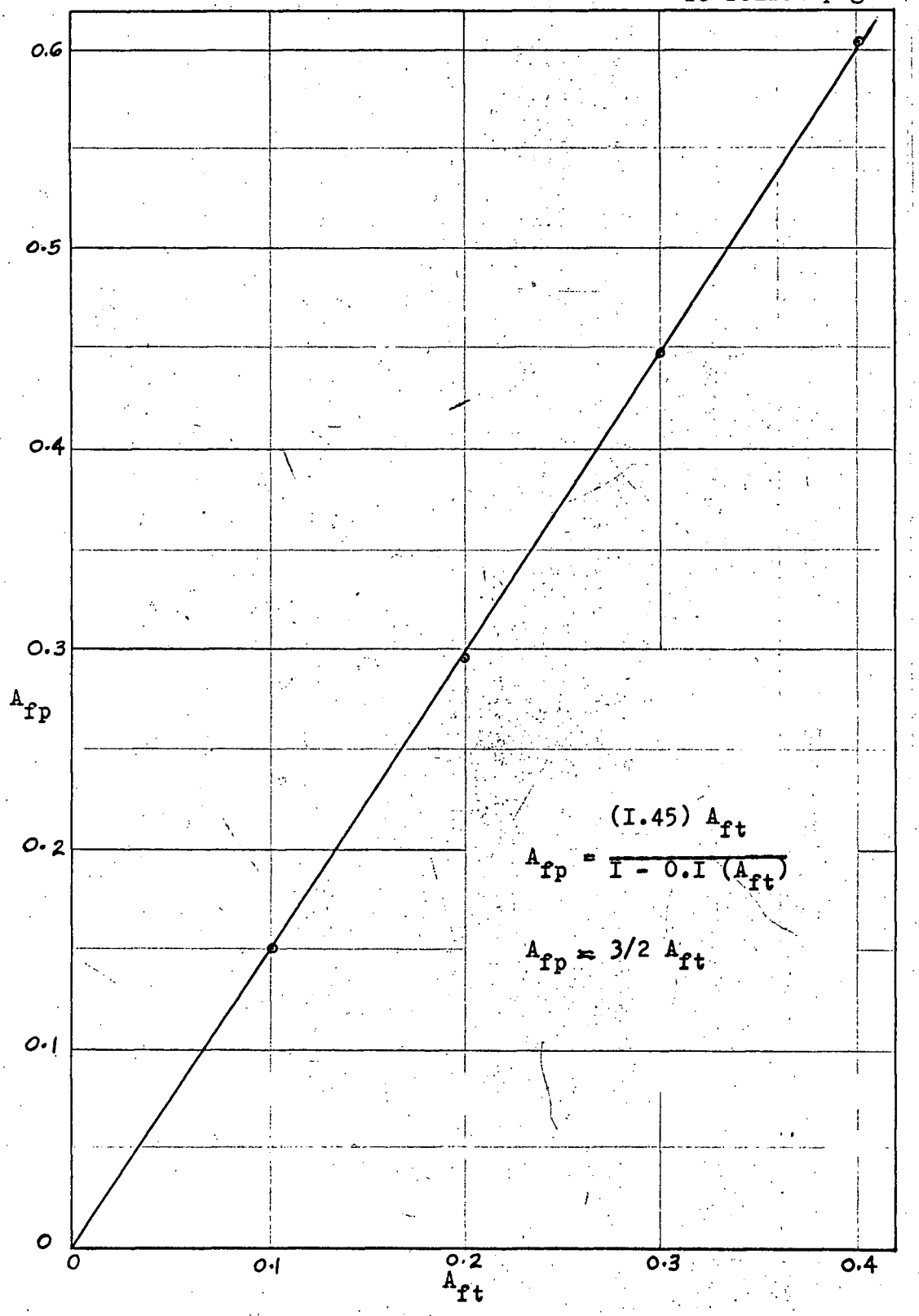

Figure - 2. EFFECT OF PLAIN STRAIN
on
PORE PRESSURE PARAMETER A_f.

this value would reduce equation (14) to

$$A_{f_p} = \frac{1.45\ A_{f_T}}{1 - .1\ A_{f_T}},$$

and figure (2) shows that this causes but a slight departure from the ideal value of 1.5 A_{f_T}. Parameter B may be expected to be substantially unaltered by a change to plane strain conditions.

(ii) U.S. Bureau of Reclamation Method

As was pointed out previously, Terzaghi (1923) showed experimentally that the effective stress was given by $\bar{\sigma} = \sigma_t - U_w$ for saturated soils. It was also mentioned that, in the case of partly saturated soils, there are two different "pore pressures" - the pore water pressure and the pore air pressure. Attention has already been drawn to the expression suggested by Bishop (1955), to give an equivalent pore pressure:

$$U = U_a - \chi\ (U_a - U_w).$$

According to Hilf (1956), however, the pore pressure is the pressure in the fluid surrounding the soil grains and furthermore, for degrees of saturation higher than about 25 per cent, the fluid surrounding the grains is the pore water. Thus, the pore pressure is equal to the water pressure in the pore space, termed pore water pressure, denoted by U_w and given by the expression:

$$U_w = U_a + U_c \quad \ldots\ldots\ldots\ldots\ldots\ldots\ldots\ldots\ (15)$$

where U_a = Air pressure in the pore space

and U_c = Pressure differential across a meniscus due to capillary forces.

With the aid of Boyle's law of compressibility of ideal gases and Henry's law of solubility of air in water an equation for air pressure in pore space

To follow page 7.

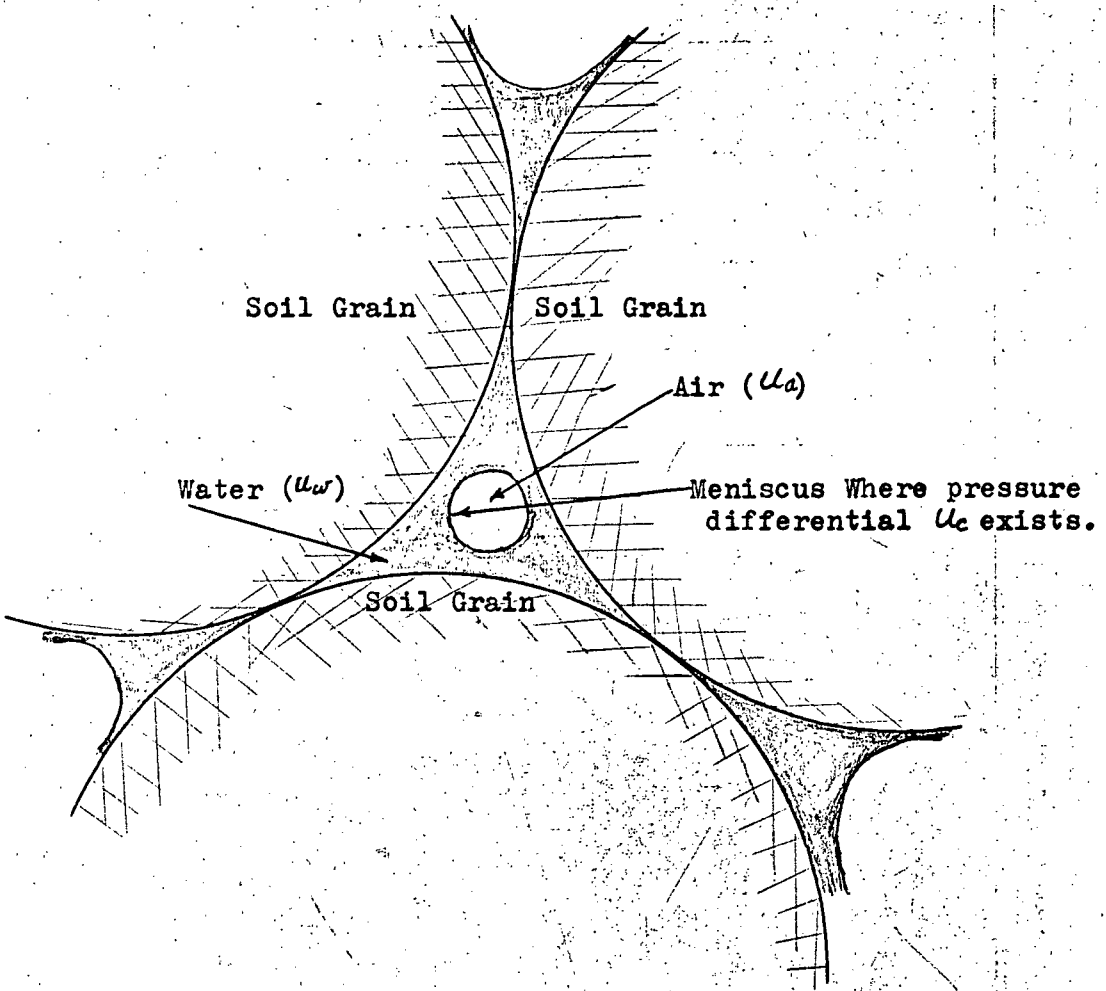

HILF'S CONCEPTION OF TWO-PHASE PORE FLUID

(for S>25%)

Figure - 3

of compacted cohesive soils has been derived by Hilf. When a load is applied to a partially saturated soil under undrained conditions the pore air is compressed and the amount of air in solution in the pore water is increased. The reduction in pore air volume is equal to the full amount of volume change in the soil. The pore air pressure developed in a compacted cohesive soil under such a load application is given by

$$U_a = \frac{P_a \Delta e}{e_{a_o} + h e_w - \Delta e} \quad \ldots\ldots\ldots\ldots\ldots\ldots\ldots\ldots \quad (16)$$

where P_a = Initial air pressure

Δe = Change in void ratio = $e_o - e_1$

e_{a_o} = Initial volume of air in soil mass of volume $1 + e_o$

e_w = Volume of water in soil mass of volume $1 + e_o$

h = Co-efficient of air solubility in water by volume

The pressure differential across a meniscus due to capillary forces, U_c, depends only upon surface tension and the radius of the meniscus, which, in turn, depends upon the radius of the pore space. The value of U_c is always negative except when the soil is saturated, the meniscus curvature is zero, and U_c is equal to zero. Thus for the degrees of saturation usually encountered in the field with compacted soils, U_c may be taken equal to zero, and then the "pore pressure" is, in fact, the pore air pressure, as given by equation (16).

Equation (16) gives pore pressure as a function of void ratio. A standard consolidation test is used to relate effective normal pressure to void ratio, and then the total pressure versus pore pressure relationship can be deduced as will be shown in the "presentation of Results". Thus pore

pressures can be predicted from total pressures without the use of the A_f and B parameters, but here stresses are again axially symmetrical. The "U.S.B.R. method", in fact, gives results for the conditions of no lateral strain in any direction.

It was mentioned that the expression for "pore pressure", U, in the case of partly saturated soils, suggested by Bishop, and used in equation (4), is a function of the pore water pressure, U_w and the pore air pressure, U_a, whereas Hilf suggests that the "pore pressure" is equal to the pore water pressure, for degrees of saturation higher than about 25 per cent. For low degrees of saturation the above two methods of evaluating the pore pressure will lead to different results. However, large positive pore pressures of practical significance will, in general, only occur at high degrees of saturation when the pore water pressure may be equated to the pore pressure with little error.

Both Bishop and Hilf agree that it is the pressure in the fluid surrounding the soil grains, which when subtracted from total normal stress gives the effective stress. Bishop believes that pore water surrounds the soil grains at high degrees of saturation but as the degree of saturation is reduced, a point will be reached when the soil particles will cease to be surrounded by the pore water, and as pointed out before the equivalent "pore pressure" will then be given by the expression:

$$U = U_a - \chi(U_a - U_w).$$

This implies that "pore Pressure" is equal to "pore water pressure", and that χ is equal to unity - till this point is reached; Hilf shows that

this point is reached at a degree of saturation of about 25 percent. If χ is equal to one for degrees of saturation higher than about 25 percent, it cannot possibly be related to degree of saturation as shown in figure (1). Hence the writer believes that Hilf is right when he equates the "pore pressure" to "pore water pressure" for degrees of saturation higher than about 25 percent.

III. SCOPE OF EXPERIMENTAL INVESTIGATION

The purpose of this investigation was to compare the pore pressure parameters measured under conditions of plane strain with those obtained from conventional triaxial tests. Other observations were also made, relative to stress-strain relationships, intermediate principal stress values and shear strength parameters (c', ϕ') in terms of effective stresses.

Standard undrained triaxial tests on cylindrical specimens were performed with pore pressure measurements, at three different chamber pressures, to determine the corresponding A_f and B values; similar tests were performed on rectangular speciments to check the influence on these parameters of specimen shape; finally, a series of tests was carried out on rectangular specimens, in which lateral expansion was prevented in one direction, to observe the effect of plane strain. The possibility of obtaining more or less uniform plane strain conditions arose from the marketing of an almost frictionless substance - Teflon - which was used as the lining material for the restraining surfaces.

The experimental investigation was limited to one silty clay and a single compactive effort at a single water content. Besides the compression tests, the index properties of the tested soil were established, compaction tests and a consolidation test were carried out.

IV. EQUIPMENT AND TEST PROCEDURES

A. Preparation of Soil Samples Used in Testing Program

The soil was obtained from Tswwassen Ferry Terminal in the province of British Columbia.

As received in the laboratory, it consists of wet, medium sized chunks, some of them partially covered with loose sand.

These chunks were washed free of the sand and were ground to pass a No. 10 U.S. Standard sieve. Water was added as a fine spray to attain the desired water contents. The soil was again passed through the No. 10 screen and was stored in gallon jars. The jars were kept stored in the humid room to prevent evaporation of moisture. This method of soil preparation provided samples that remained at essentially constant water content for the period of this investigation. The soil was allowed to cure for a minimum period of 24 hours before compaction. In some cases, soil was reused: test specimens (which had lost some water during handling, but had never been oven-dried) were reground and re-moistened for subsequent tests.

B. Compaction Tests

Standard Proctor compaction gave an optimum water content of 20.0% and a maximum dry density of 107.0 lbs./cu.ft. The intention was to devise compaction procedures which would give test specimens with a maximum dry density of the order of 95% to 100% of the maximum dry density for Standard Proctor compaction.

(i) Cylindrical specimens

Cylindrical samples were compacted with the Harvard Miniature apparatus (1)

---

(1) "Small soil compaction apparatus duplicates field results closely", by S.D. Wilson, Engineering News Record, November, 1950, pp. 34 - 36.

which utilizes a mold having a volume of $\frac{1}{454}$ cu.ft. and a tamper of $\frac{1}{2}$ in. tip diameter. All specimens were compacted in 5 layers, 25 tamps per layer with a stressed spring tamper set to 20 lbs. Optimum water content of 20.0% and a maximum dry density of 103.0 lbs./cu.ft. were obtained. This was considered satisfactory. All specimens were nominally 2.816 in. long and 1 5/16 in. in diameter.

(ii) Rectangular Specimens

Description of Apparatus (2) - The rectangular compaction equipment is illustrated in Fig. 4. The compaction mold and extension collar were made from $\frac{1}{4}$ in. aluminum plates. The mold was 3 in. long and 1.272 in. by 3.50 in. in horizontal cross section. Its volume was .00773 cu.ft. The $\frac{1}{2}$-in. brass base plate, the mold and the extension collar were held in place as shown in Fig. 4a while the soil was being compacted.

The tamper was essentially the same as the Harvard Miniature Compactor except that it had a square tip to give the same tip area as that of the round rod of $\frac{1}{2}$ in. diameter.

The extension collar was split into four plates; and the plates were removed from the compacted soil one at a time. This avoids shearing off the specimen and gouging below the level of the top of the mold.

Similarly, the mold was taken apart and the plates were peeled off the compacted specimen one at a time. Hence the compacted specimen was removed from the mold quite conveniently and with little disturbance. Disturbance was cut down to a minimum if the mold plates were coated with a

(2) The apparatus used for rectangular specimens was designed and constructed in the workshop of Dept. of Civil Eng., University of British Columbia.

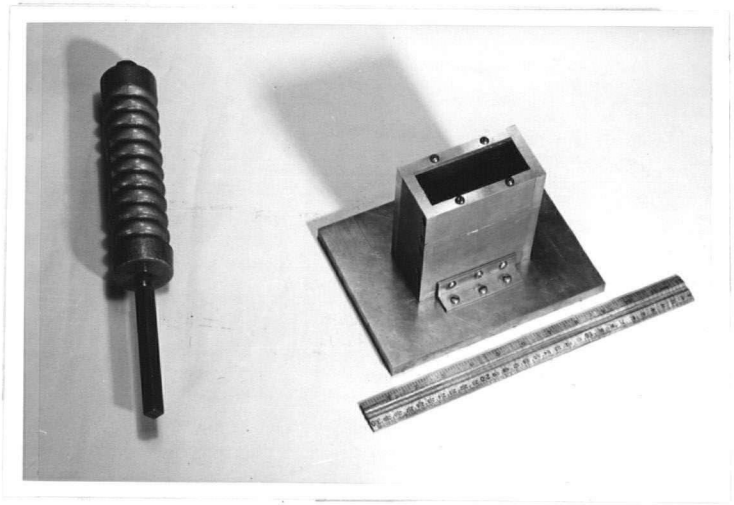

(a)

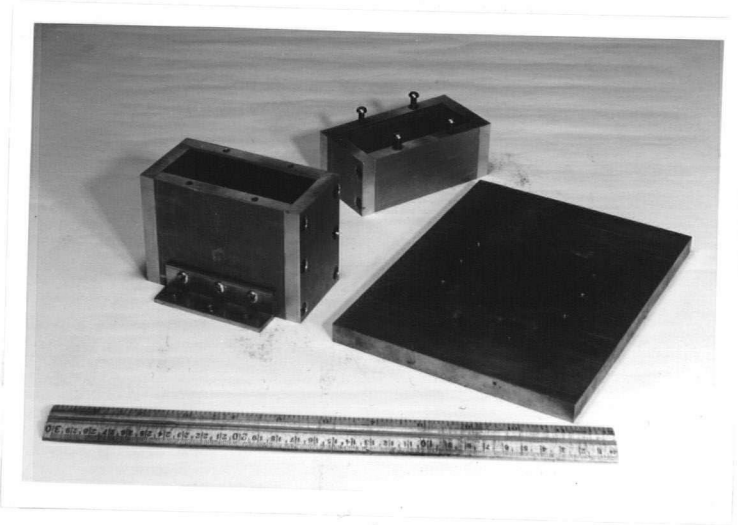

(b)

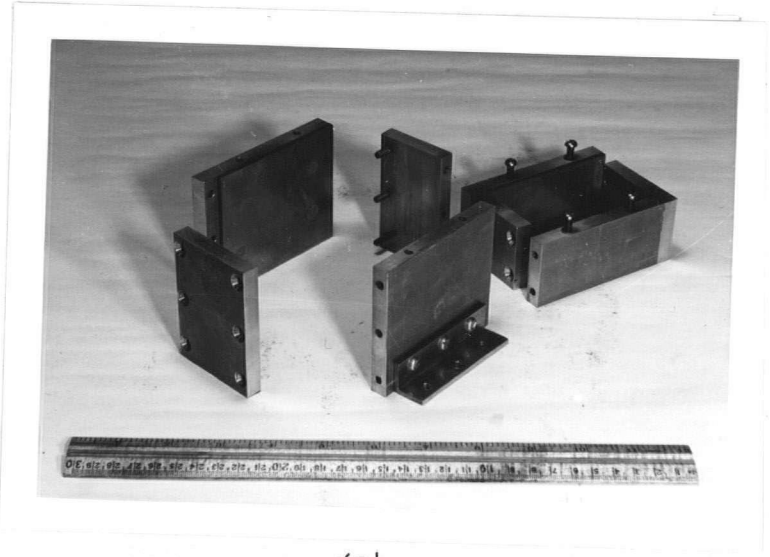

(c)

Fig. 4 Compaction equipment used for rectangular specimens

To follow page 13

thin film of oil before the compaction was started.

Experimental Procedure - The rectangular specimens were compacted with different compactive efforts for a water content of 20.0%.[3] The specimens compacted in 5 layers, 40 tamps per layer with a stressed spring tamper set at 30 lbs.had,[4] within the experimental accuracy, the same dry density as that obtained in the case of cylindrical tests.

C. Undrained Triaxial Tests with Pore Pressure Measurements

(i) General Equipment

A strain-controlled triaxial machine was used for all tests reported herein. Axial stress was applied to the specimens by means of an electrically driven "Transmission Unit" which actuates the loading screw through a chain drive. A "Proving Ring Assembly" and "Specimen Loading Yoke" are attached to the loading screw. To attain the desired rates of axial strain, a speed control dial is connected, through a flexible shaft, to a variable speed clutch included in the transmission unit.

A pore pressure panel based on the Massachusetts Institute of Technology design, was used in all tests reported herein. The pore pressure measuring device was a non-flow null indicator in which back pressure is applied to the pore water in order to prevent moisture movements from the test specimen. The magnitude of the back pressure is deemed to represent

---

(3) Optimum water content as found in cylindrical tests and Standard Proctor Compaction.

(4) The purpose of this test was to find the Compactive effort required to get the dry density for rectangular specimens equal to that obtained in case of round specimens.

the pore pressure at the location in the specimen where the back pressure is applied. The procedure used in the investigation pertains to pore pressure measurements at the bottom of the specimen. Before new apparatus, or one that has not been used for some time, can be put to use, it is absolutely essential to make sure that the system is free of air and that all the lines are full of de-aired water. This problem is discussed next.

De-airing of Pore Pressure Apparatus - The complete layout for de-airing of the apparatus is shown diagrammatically in Fig. 5. The de-airing procedure is outlined below:

(1) With valves 1,2,3,4 and 6 open, and the rest of the valves shut, vacuum is applied to the system till the compound pressure and vacuum gauge reads 30 in. Hg.

(2) Valve 4 is shut and by opening valve 5 water is drawn from the tank, through the system, into the reservoir in the pore pressure panel. While the water is being drawn through the system, rapid closing and opening of valves 1,2 and 3 facilitates the removal of air from the valves themselves.

(3) When the reservoir is full valve 3 is closed. Rapid opening and closing of valve 4 removes air from the valve itself.

(4) To check that the system is now air-free, valves 1 and 6 are closed, and valve 4 is open, with valve 7 temporarily open to get a convenient level in the glass tube while there is a positive pressure in the Pressure Equilizer Tank. The pressure gauge indicates an initial reading.

To follow page 15.

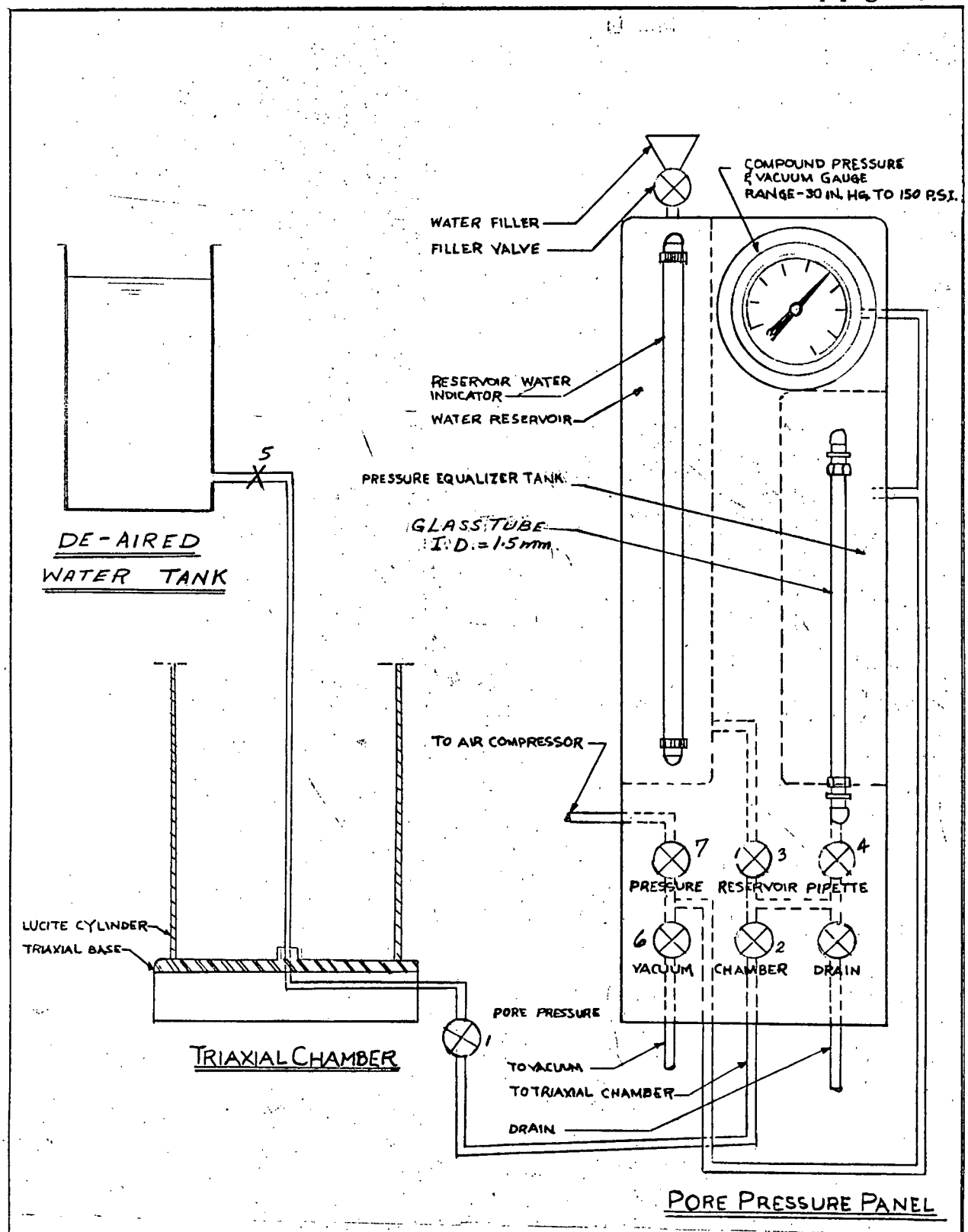

Figure-5. A Schematic Diagram To Show The Layout For De-airing of Pore Pressure Measuring Apparatus.

(5) Pressure is increased by opening valve 7. A drop in the water level in the glass tube indicates either expansion of the apparatus, compression of air bubbles still remaining in the system, or leakage. If the valve 7 is adjusted to maintain constant pressure in the pressure equilizer tank, steady creep of the water level indicates leakage. A large drop which is not fully reversible generally indicates air bubbles, which pass into solution at higher pressures.

A fully reversible drop in level of less than ½ in. per 50 lb./sq. in. rise in pressure should readily be achieved. To get greater accuracy, the zero line used in the null method is adjusted progressively with change in pressure to allow for this deflection.

This elaborate de-airing procedure is seldom necessary once the apparatus is in regular use. It is generally sufficient to check the system prior to each test by a momentary increase in pressure.

(ii) Special Equipment(5)

Rectangular Triaxial Tests - The main special equipment required included a rectangular pedestal, a rectangular loading head and a rectangular porous stone.

Later on it was found difficult to seal the rectangular specimen inside the membrane since the circular "O"-rings did not provide enough normal pressure along the sides of the rectangular pedestal or the rectangular loading head to seal the membrane to the end fittings. The side fittings, as shown in figure (6), were designed to press against the "O"-rings and thus develop the normal pressure necessary for a pressure tight seal.

---

(5) All equipment refered to under "Special Equipment", was designed and constructed in the workshop of Dept. of Civil Eng., University of British Columbia.

To follow page 16

(a)

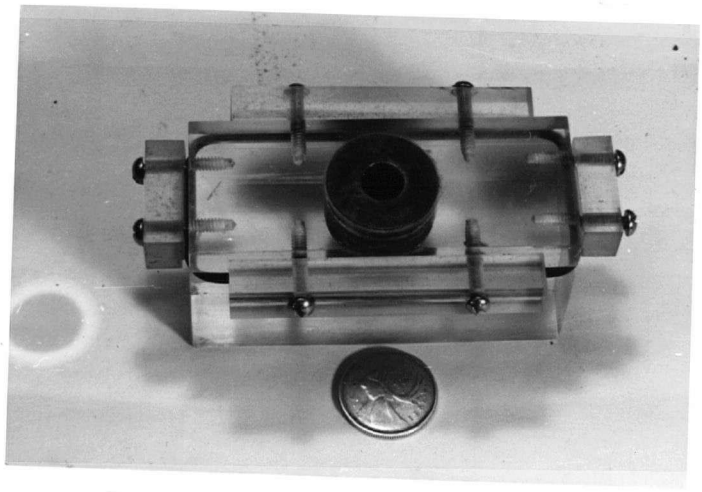

(b)

Fig. 6 Special Equipment for Rectangular Triaxial Tests.

To check that the membrane could now be sealed to the end fittings, a dummy specimen, made of wood, was set up in the triaxial cell. The specimen and the end fittings were coated with the paste called "McCabes - Water level indicator"[6]. A rubber membrane protected the wooden block from the chamber fluid (in this case, de-aired water). The "O"-rings and side fittings were used to seal the membrane to the end fittings. A chamber pressure of 75 lb/sq.in. was applied for a period of 24 hours. At the end of this time, the block was carefully removed from the cell and examined for any evidence of leakage through the membrane or end fittings. No change in colour of the paste was observed, so it was concluded that the protective measures were adequate.

Plane Strain Apparatus - When all the strains in a body are parallel to a given plane, the body is said to be in a state of plane strain. In this case, an attempt is made to design and construct special plane strain equipment which allows strains only in the direction parallel to the intermediate principal plane (plane perpendicular to σ_2 as shown in Fig. 7).

The plane strain apparatus, as shown in Fig. 8, consists of two $\frac{1}{2}$-in. thick, 1.5 in. by 3.25 in. rectangular plates which could be assembled by means of four side bars to form a rectangular frame. This plane strain frame is 3.25 in. high and could be varied in length from 3.50 in. to 3.60 in. (The dimensions are from inside to inside.) But, once locked at a certain length, the frame could maintain that length throughout the test, thus preventing lateral expansion in one direction.

---

(6) "McCabes - Water level indicator" is widely used by the petroleum industry to detect water in gasoline. It is green in colour and turns bright scarlet on contact with moisture.

To follow page I7.

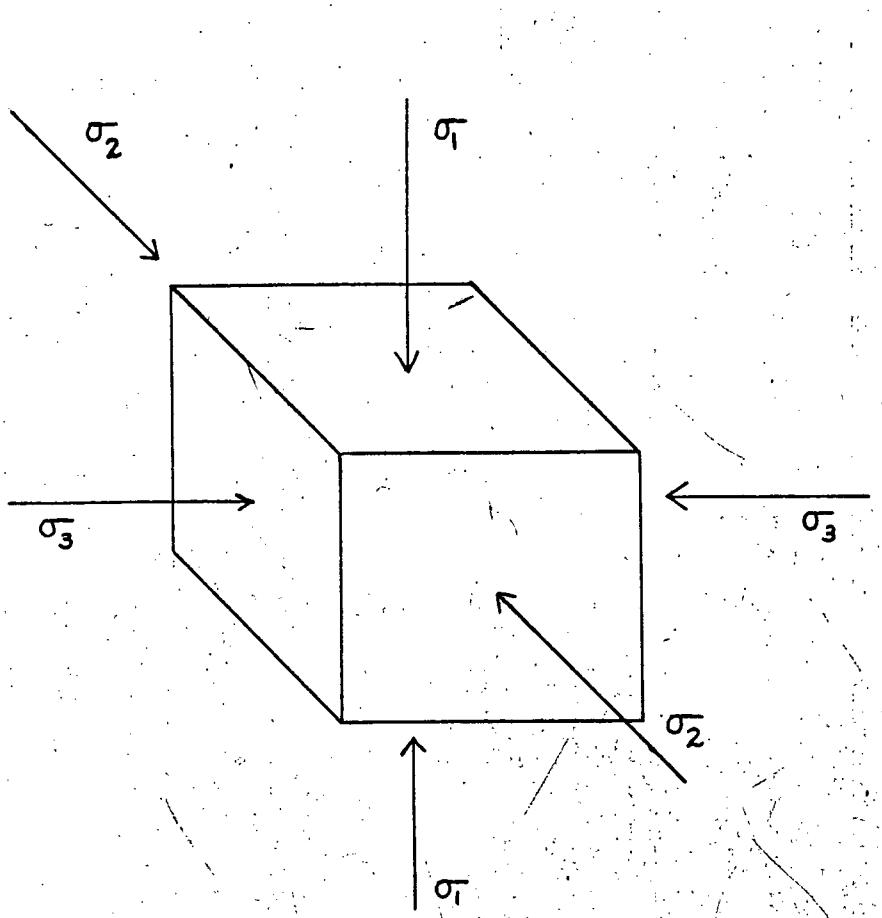

ELEMENT UNDER PRINCIPAL STRESSES

FIGURE - 7

To follow page 17

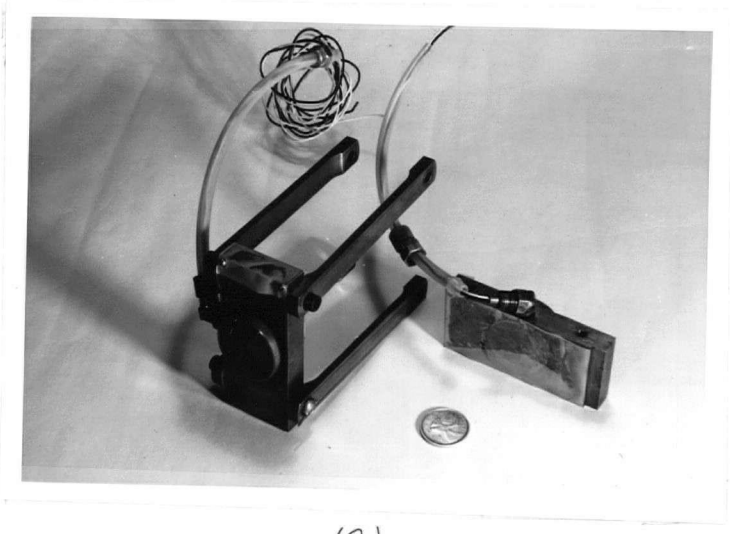

(a)

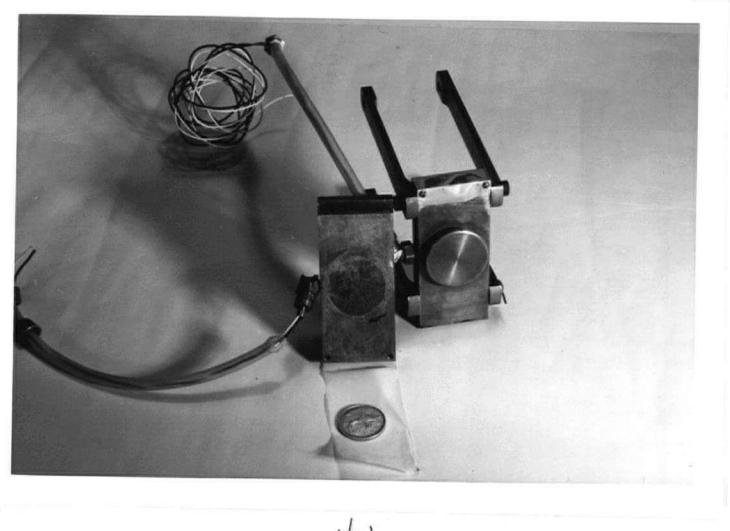

(b)

Fig. 8 Plane Strain Apparatus

If the plane strain frame as described in the above paragraph was used in the tests, the brass plates would have to be in contact with the soil specimen. Thus during the shearing phase of the test an unknown friction force would develop between the soil specimen and the brass plates. This unknown friction force would affect the load dial readings and the true value of the deviator stress would be hard to determine. Lateral expansion in the σ_3 direction would also be inhibited near the σ_2 ends of the specimen, so that the assumed conditions of uniform stress would not be obtained.

To cut the friction to a minimum, the inside face of each brass plate was lined with .005 in. thick Teflon tape; the co-efficient of friction for Teflon against soil contained in a rubber membrane was later found to be .05. The Teflon tape was secured on the back of the brass plate by means of two screws, as shown in figure (8), and then it was rolled over the top of the plate to cover the inside face of the plate. A thin film of vacuum grease on the inside face of the plate helped to keep the tape in place.

It was later decided to mount an electrical pressure transducer in the brass side plates and to measure the intermediate principal stress, σ_2, throughout the test. Now, since σ_2 was to be measured the value of the friction force could be calculated at any stage of the test and the load dial readings could be corrected accordingly to give the true average value of the deviator stress.

A hole 7/8 in. diameter was drilled in the centre of the plate; an extra groove .020 in. deep was provided all around the 7/8 in. hole to give an

opening of one in. diameter in the inside face of the plate. Basically, the transducer consists of one in. diameter pressure sensing diaphram made of Beryllium Copper. The diaphram was heat treated at 600°F and was soft soldered into place to give an even surface with the inside face of the brass plate.

One 120 - ohm Metal film strain gauge (7) was glued onto the back of the diaphram. The electrical wires from the strain gauge were taken out of the recess behind the diaphram through an aperture in the side of the brass plate. As shown in figure (9), the back of this recess was sealed by means of an "O"-ring. The electrical wires were enclosed inside "Imperial poly-flow" tubing as they emerged from the side of the plate and provision was made for the wires to be taken out of the triaxial cell through an opening in the base of the cell. Proper end fittings were provided for the tubing so that the recess behind the diaphram would be sealed from the triaxial chamber fluid and still be open to atmospheric pressure; hence the reference pressure was atmospheric. The free ends of the electrical wires were connected to a "Baldwin Strain Indicator", which read a unit strain in micro inches per inch. An application of pressure caused the diaphram to deflect and actuated the strain gauge which produced a reading on the strain indicator.

The transducer could be calibrated quite simply in the triaxial cell by direct application of water pressure on the diaphram.

---

(7) It was Type C6 - 141 - B
Manufactured by "The Budd Company",
P.O. Box 245, Phoenixville, PA.

To follow page I9.

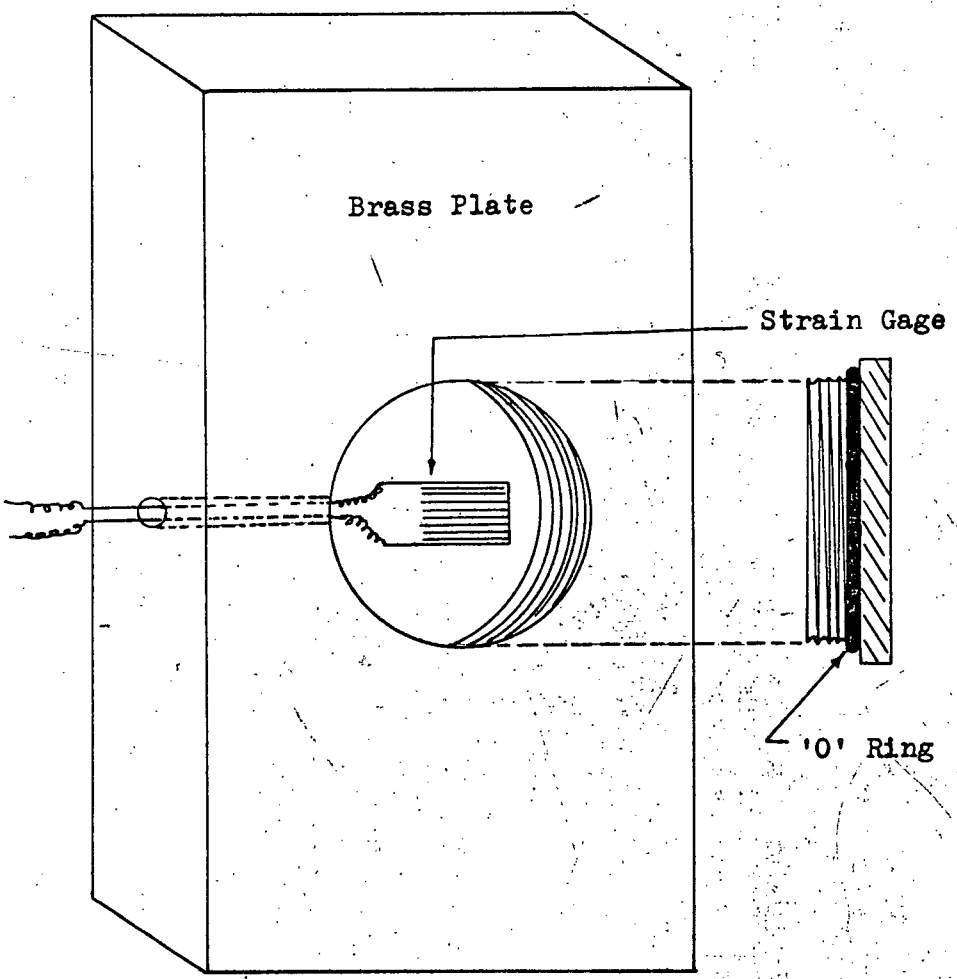

Figure - 9. A Schematic Diagram
of
The Transducer.

(iii) Testing Procedure

Cylindrical Triaxial Tests - Three tests were performed at each of three different cell pressures - 30 psi, 60 psi and 75 psi. Thus, this series consists of nine tests.

All specimens were compacted to maximum dry density at optimum water content. The compacted specimens were extruded from the compaction mold and were placed in the triaxial chamber in the manner described in "Soil Testing for Engineers" by T.W. Lambe. Only one porous stone was used. The porous stone was saturated prior to the test and was placed on the pedestal. Every precaution was taken to make sure that no air bubbles were entrapped between the porous stone and the pedestal.

Excess water, if any, was very carefully removed from the pedestal and the porous stone. It was found quite convenient to roll the rubber membrane over the specimen and "O"-rings were used to seal the specimen.

The stress changes were made in two stages: (i) an increase in the cell pressure resulting in a uniform all-round change in stress and (ii) an increase in axial load resulting in a change in deviator stress. The cell pressure was applied using de-aired water as chamber fluid, in six increments at the rate of an increment every five minutes. The pore pressure was recorded for every increment in cell pressure. Thus, it took half an hour to apply the required cell pressure. The uplift on the piston due to the cell pressure was counterbalanced by means of dead weight. Axial loading (deviator stress) was applied at an average rate of about .27% axial strain per minute. A dial gauge reading in $\frac{1}{1000}$ in. divisions was used to measure deformation. Readings of the load dial and pore pressure were taken at intervals of 20 divisions for the first 100 divisions, at intervals of 40 divisions for the next 200 divisions and at every 100 divisions after that.

To follow page 20

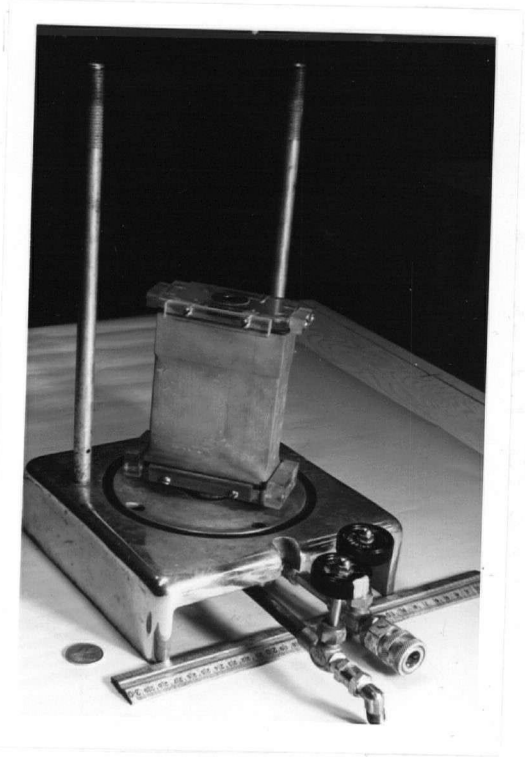

Fig. 10 A Rectangular Specimen in place

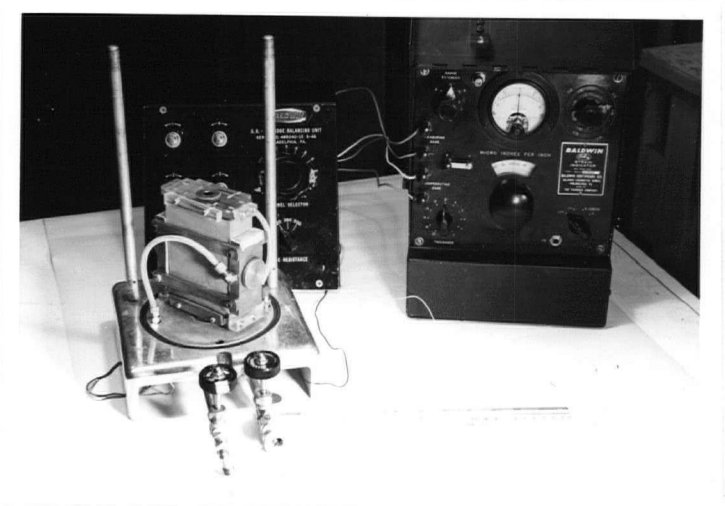

Fig. 11 A specimen assembled for a plane strain test

Rectangular Triaxial Tests - This series of tests also consisted of nine tests - three tests at each of the cell pressures, 30 psi, 60 psi and 75 psi. The test procedure followed was similar to that used in Cylindrical Triaxial Series - the only difference being that the average rate of axial strain was .23% strain per minute.

Plane Strain Tests - This series of tests again consisted of nine tests. The specimen was set in the triaxial chamber in a manner similar to that used in the Rectangular Triaxial Series. (See Fig. 10) Before assembling the triaxial chamber, the plane strain apparatus was put in place as shown in Fig. 11. The length of the plane strain frame was adjusted in a manner such that the "Strain Indicator" showed a positive deflection, indicating that the plane strain plates were in contact with the soil specimen. The testing procedure followed was the same as that used in the case of the "Rectangular Triaxial Series".

To follow page 21

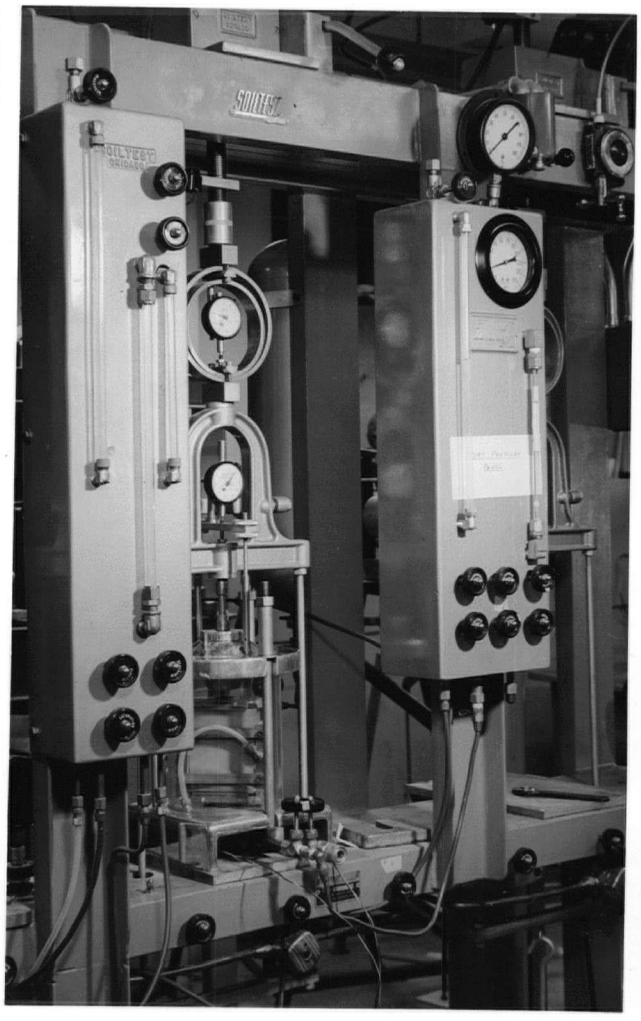

Fig. 12 A specimen set up in the triaxial machine for a plane strain test

V. PRESENTATION OF RESULTS

A. Soil Data

The pertinent data on the soil used in this investigation are given below in Table I.

TABLE I

SOIL PROPERTIES

Specific gravity	2.69
Liquid Limit	36.4%
Plastic Limit	29.2%
Plasticity Index	7.2%

The grain size curve for the soil along with the M.I.T. Classification scale is presented in Fig. 13.

B. Presentation of Results

The results of the tests for this investigation are mostly presented in graphical form for ease in visualizing trends quickly and accurately. The points used for determining the curves are shown where applicable.

In Fig. 14 are presented graphs of "Dry density versus Molding Water Contents" for Standard Proctor Compaction and Harvard Miniature Compaction tests. Lines representing degrees of saturation of 80%, 90% and 100% are also given in Fig. 14.

Figs. 15 - 17 show average stress-strain curves (1) for three different cell pressures for all three series of tests. The average as-molded conditions, (2) for all three series of tests, are given in Table II.

(1) For stress-strain curves of individual tests, see Figs. 32 - 40 in Appendix I.

(2) For As-molded conditions for individual tests see Table VI in Appendix I.

TABLE II

AVERAGE AS-MOLDED CONDITIONS

SERIES OR TYPE OF TESTS	CELL PRESSURE p.s.i.	AVERAGE MOLDING WATER CONTENT %	AVERAGE DRY DENSITY lbs/Cu.ft.	AVERAGE SATURATION %
CT	30	20.02	102.3	84.8
	60	20.30	103.3	87.9
	75	20.02	102.6	85.3
RT	30	20.31	103.3	86.7
	60	20.20	104.1	89.2
	75	20.30	104.0	88.9
PS	30	19.98	104.1	87.9
	60	20.00	103.8	87.0
	75	19.91	104.6	88.6

Graphs of average pore pressure parameter B (3) versus cell pressure and secant modulus of deformation M_{50} (corresponding to 50% of the average maximum deviator stress) versus cell pressure are plotted in Figs. 18 and 19 respectively.

In Fig. 20 is plotted the average pore pressure parameter A_f (4), for three different criteria of failure (maximum deviator stress, maximum effective principal stress ratio and 10% axial strain), as a function of cell pressure (σ_3), for all three series of tests.

---

(3) The B-values for all individual tests are given in Table VII in Appendix I.

(4) The A_f-values for all individual tests are given in a tabulated form in Table VIII in Appendix I.

Figs. 21 - 23 are plots of Mohr circles (in terms of total stresses), for average maximum deviator stress for a cell pressure.

Typical pore pressure prediction curves by "U.S. Bureau of Reclamation Method" are given in Fig. 24. The curve e versus $\bar{\sigma}$ is drawn on the basis of a consolidation test and the curve e versus U_w is drawn with the aid of Hilf's formula,

$$U_w = \frac{P_a(e_1 - e_2)}{(V_a + HV_w)(1 + e_1) - (e_1 - e_2)}$$

where the symbols are the same as used previously. The other curves are drawn by combining the plots of e versus $\bar{\sigma}$ and e versus U_w.

In Figs. 25 - 27 are plotted the Mohr circles (in terms of effective stresses) on the basis of maximum deviator stress.

The vector curves (or effective stress paths) for all individual tests are plotted in figures 28 - 30. They show the changing relationship between shear stress and effective normal stress on the potential failure plane, throughout the tests. They were computed on the assumption that the potential failure plane was inclined at 60° to the major principal plane, assuming a friction angle of 30 degrees.

The calibration curves for the transducers used in the plane strain apparatus are given in Fig. 31. The results of the friction tests to determine the co-efficient of friction of teflon against the soil contained in a rubber membrane are given below in Table III.

TABLE III

FRICTION TESTS ON TEFLON

NORMAL LOAD	PROVING RING DIAL READINGS IN .0001"				FRICTION FORCE	CO-EFFICIENT OF FRICTION
lbs	Test No.					
	1	2	3	Average		
53	8.0	7.0	8.0	$\frac{23}{3}$	$.32(\frac{23}{3}) = 2.45$	$\frac{2.45}{53}$ .05

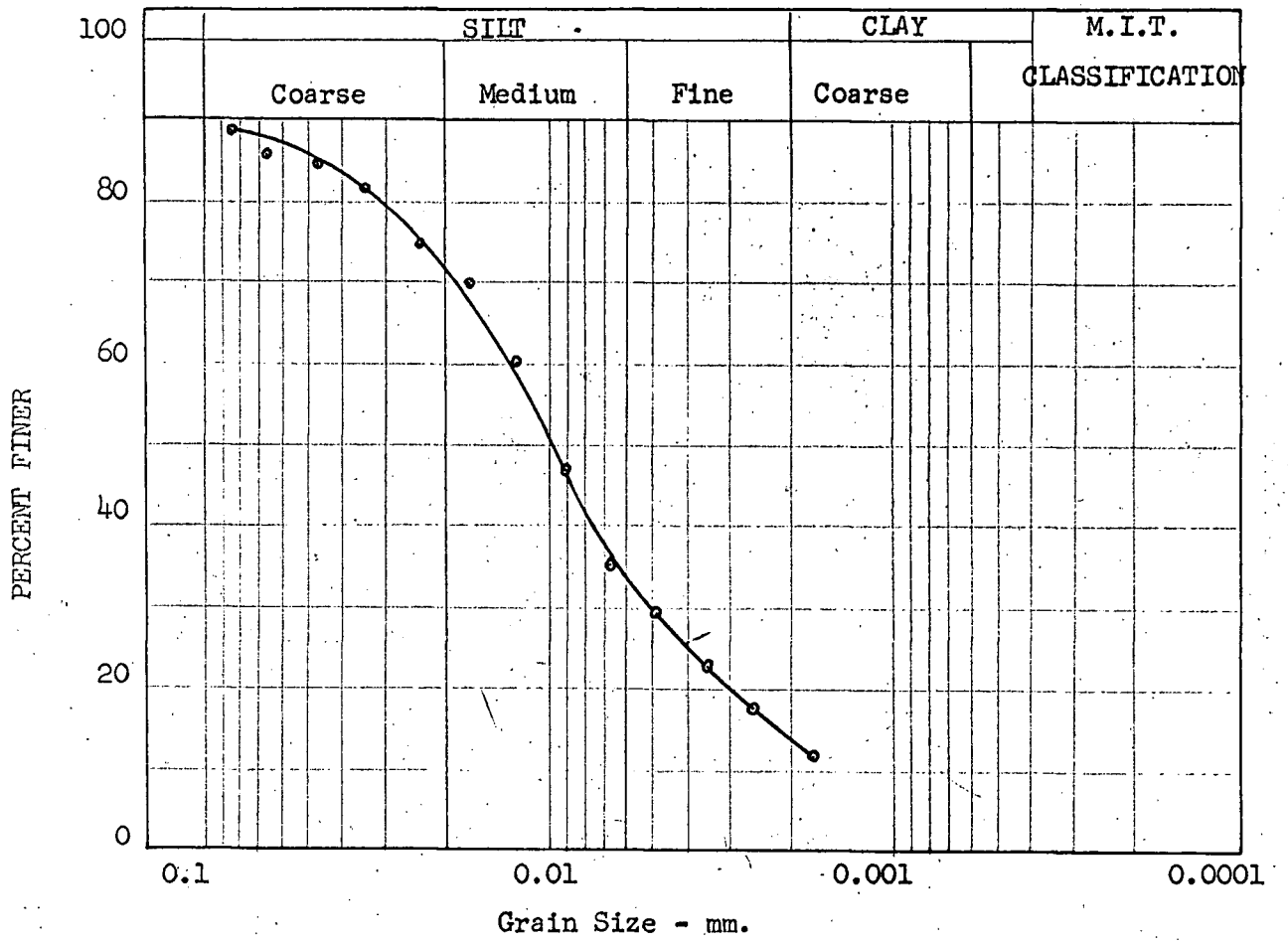

FIG. 13 - GRAIN SIZE CURVE

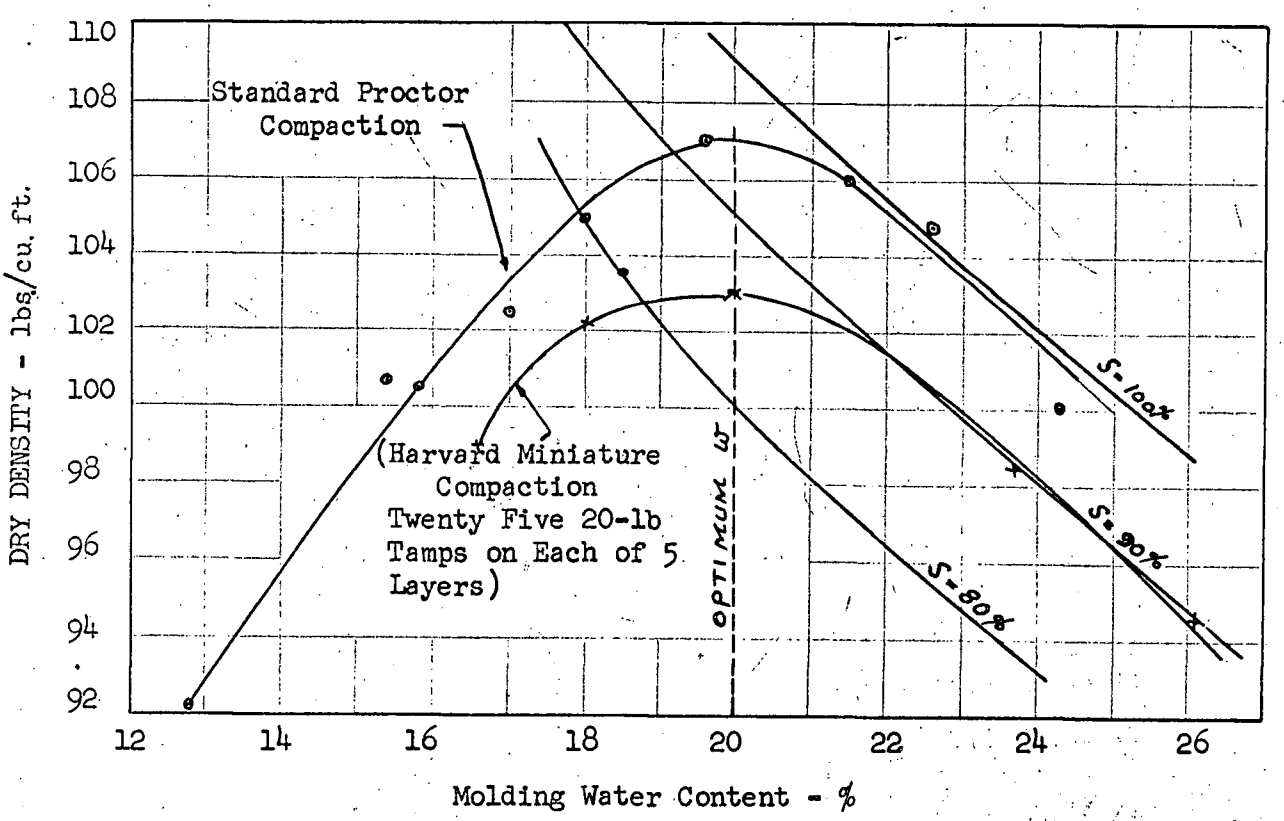

FIG. 14 - COMPACTION CURVES

To follow fig. 14

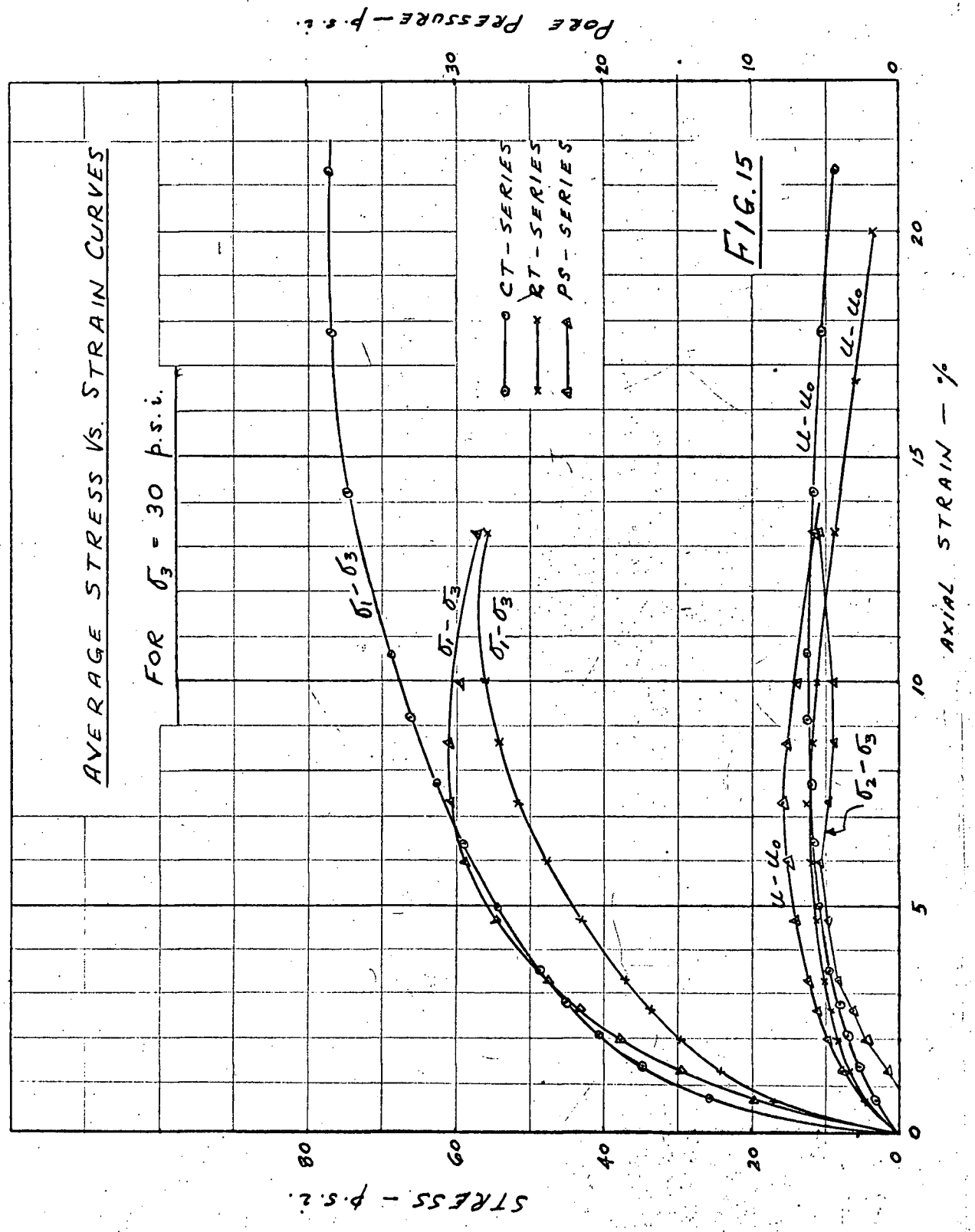

FIG. 15

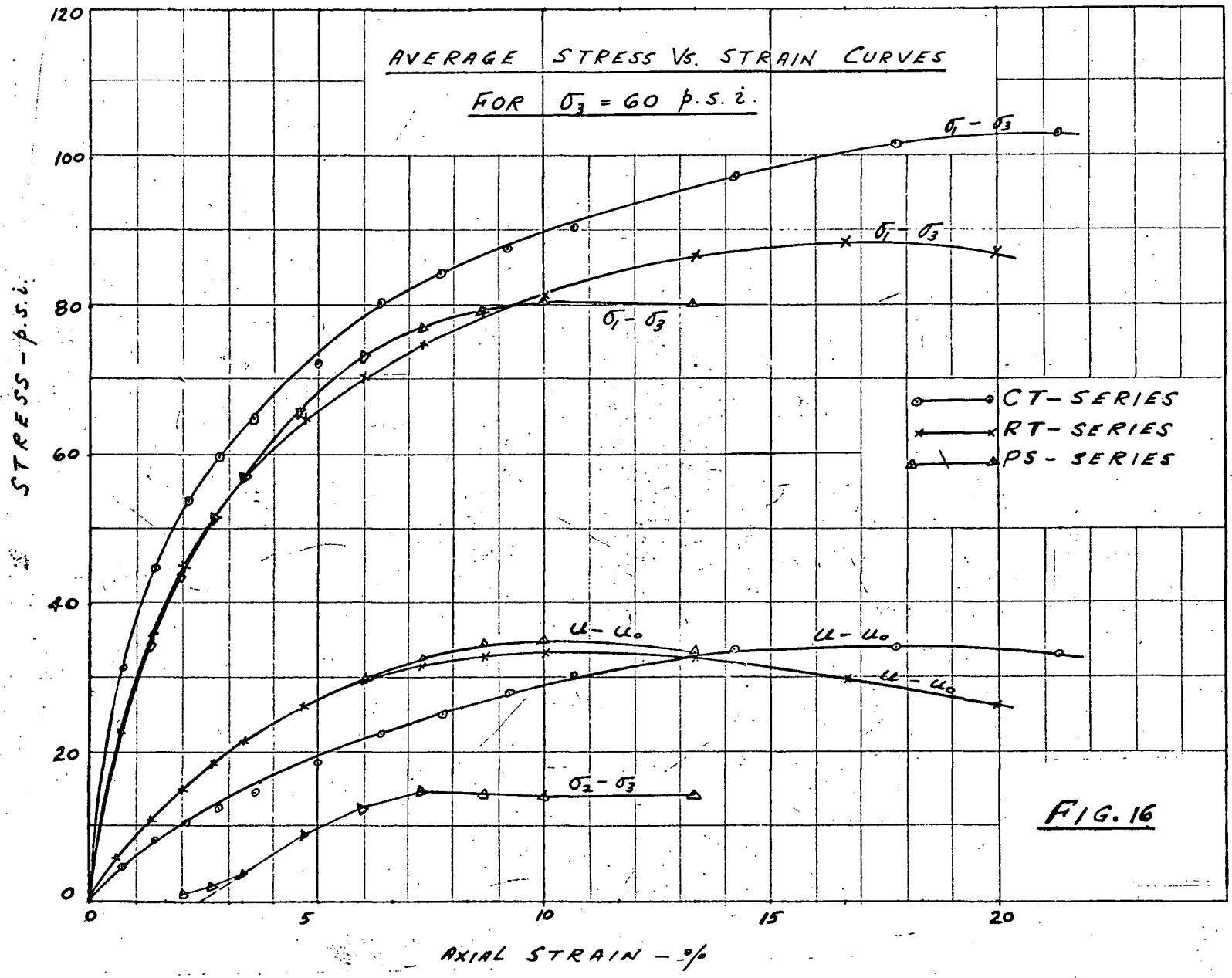

FIG. 16

To follow fig. 15

To follow fig. 16

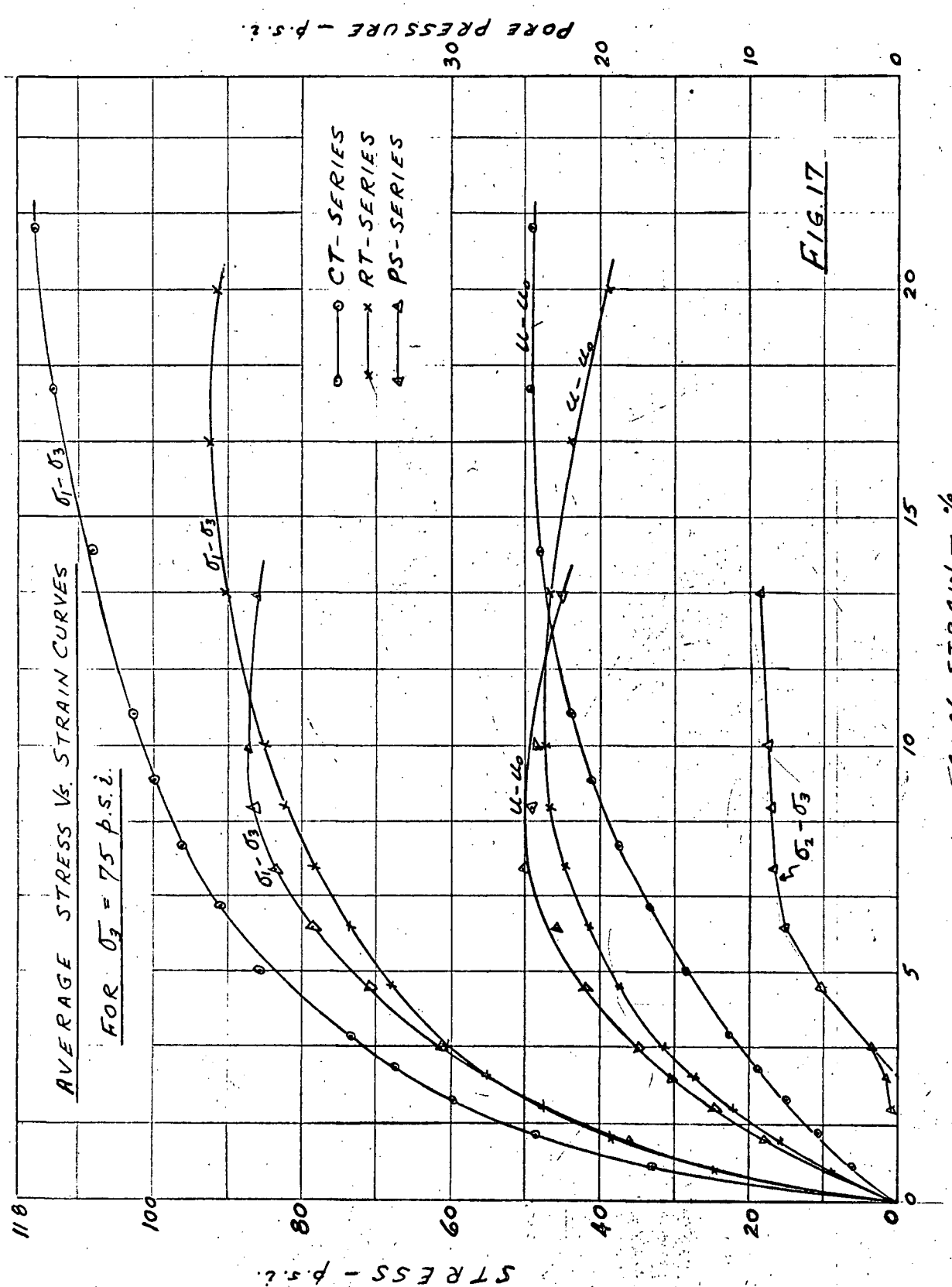

FIG. 17

To follow fig. 17.

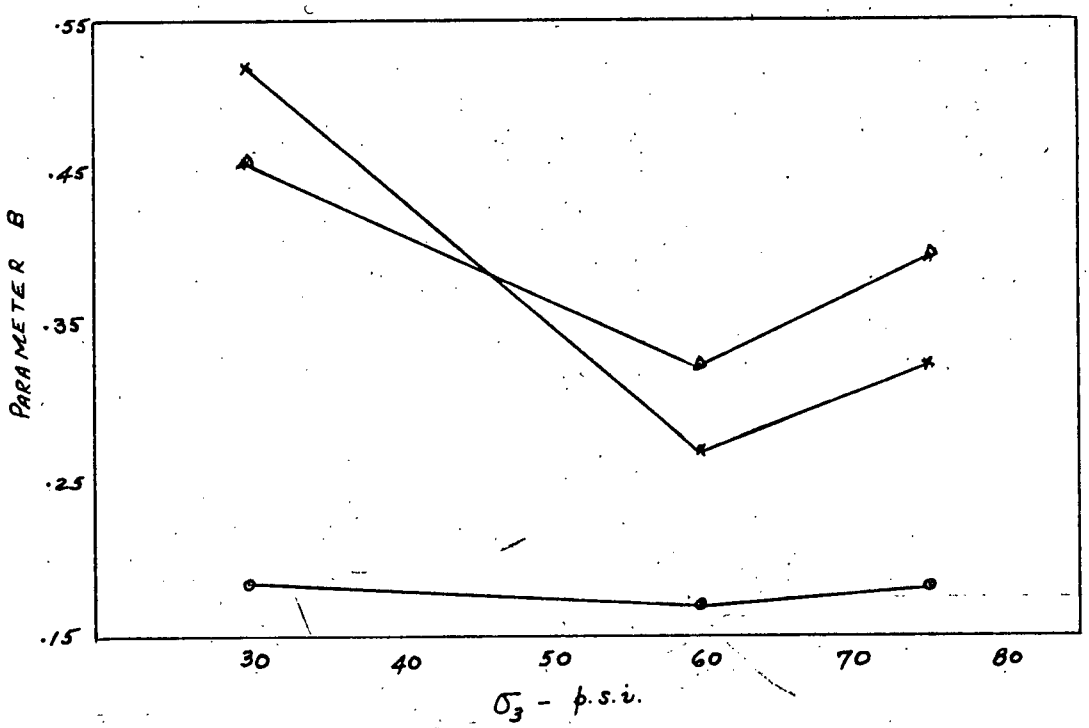

FIG. 18 - PARAMETER B

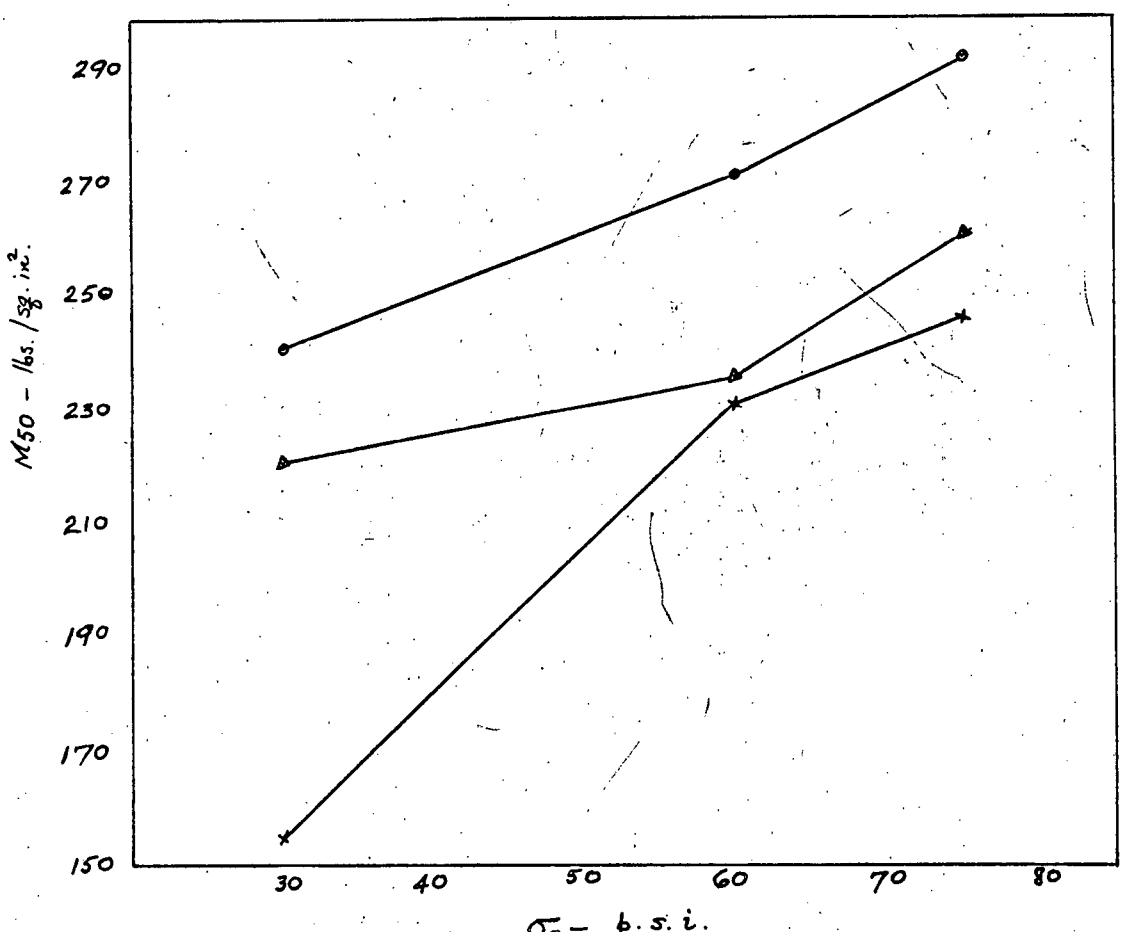

FIG. 19 - SECANT MODULUS OF DEFORMATION (M50).

FIG.20- PORE PRESSURE PARAMETER A_f VERSUS CELL PRESSURE

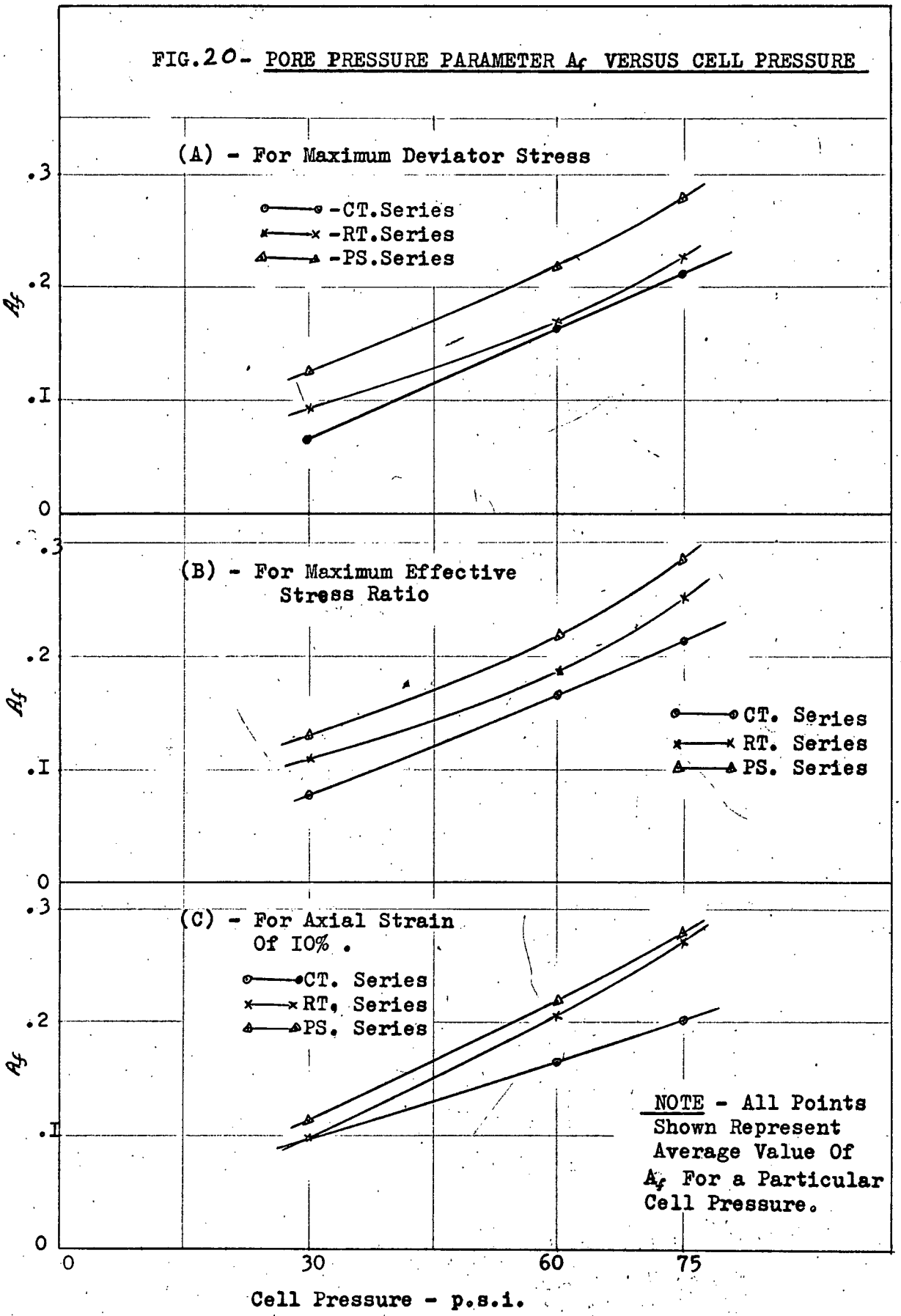

Figure - 21. Mohr Circles of total stresses for Maximum Average Deviator Stress
CT - Series

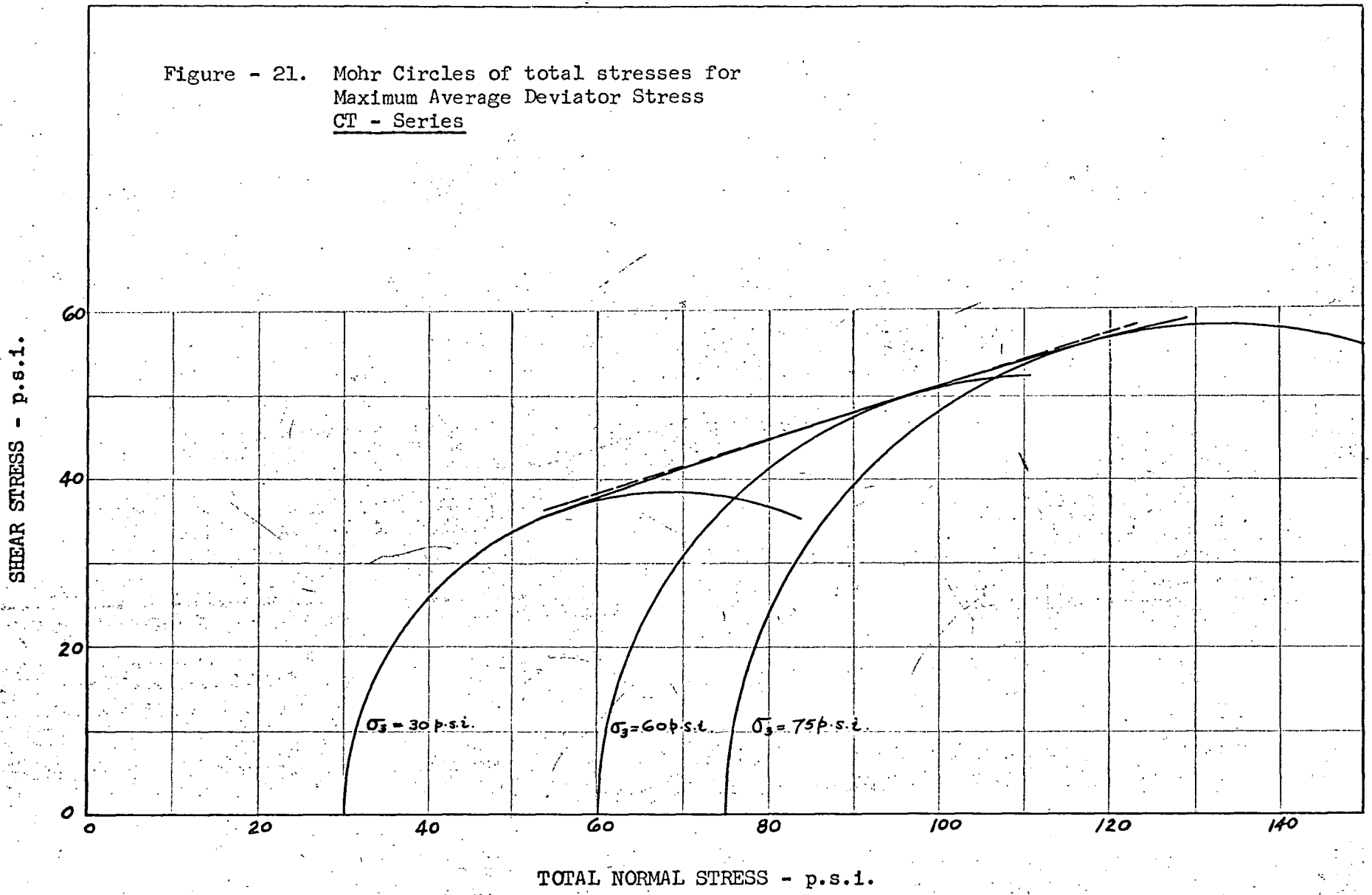

To follow Fig. 20

Figure 22 Mohr Circles of total stresses for
Maximum Average Deviator Stress
RT - Series

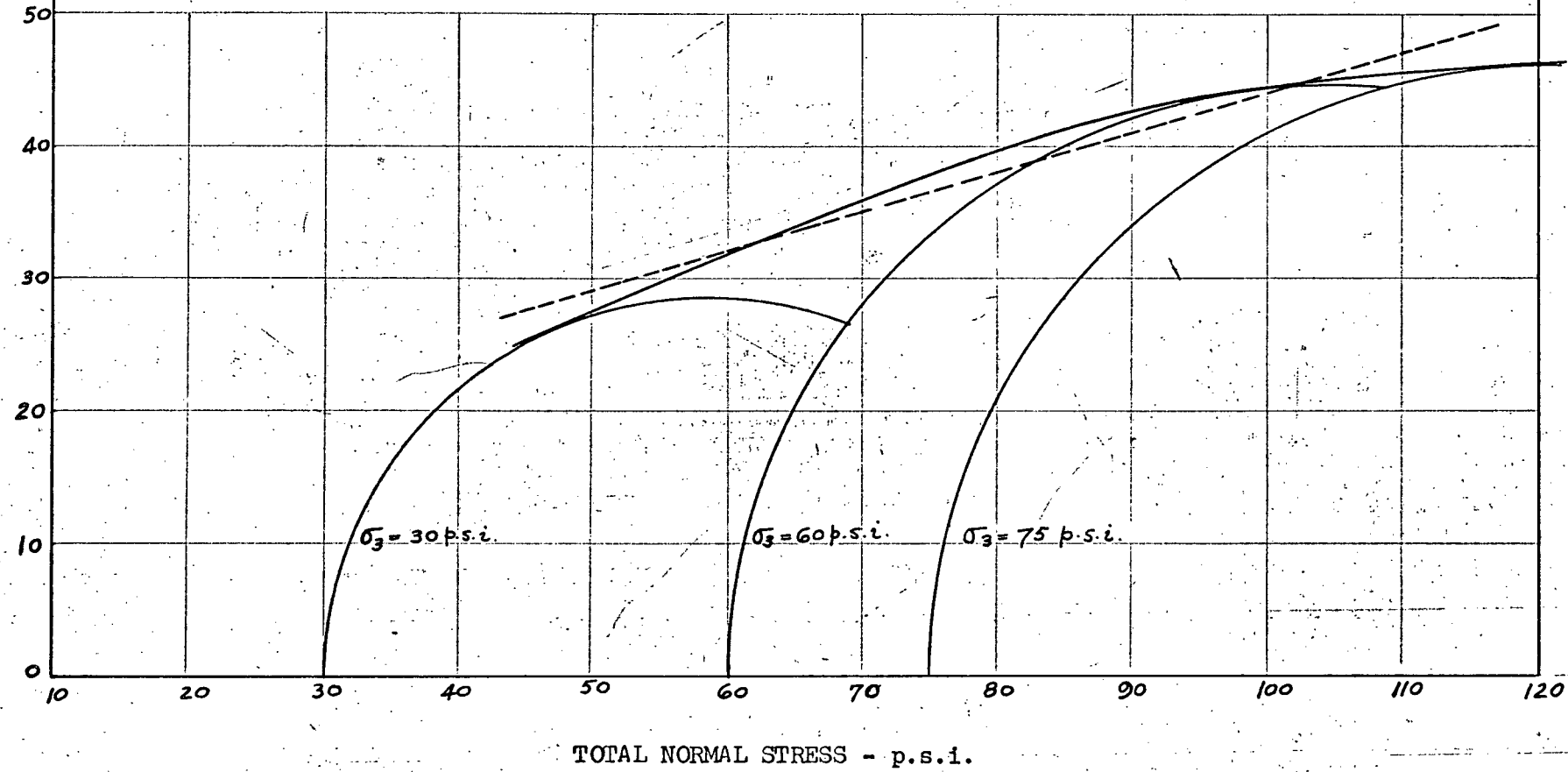

To follow Fig. 21

Figure - 23 Mohr Circles of total stresses for
Maximum Average Deviator Stress
PS - Series

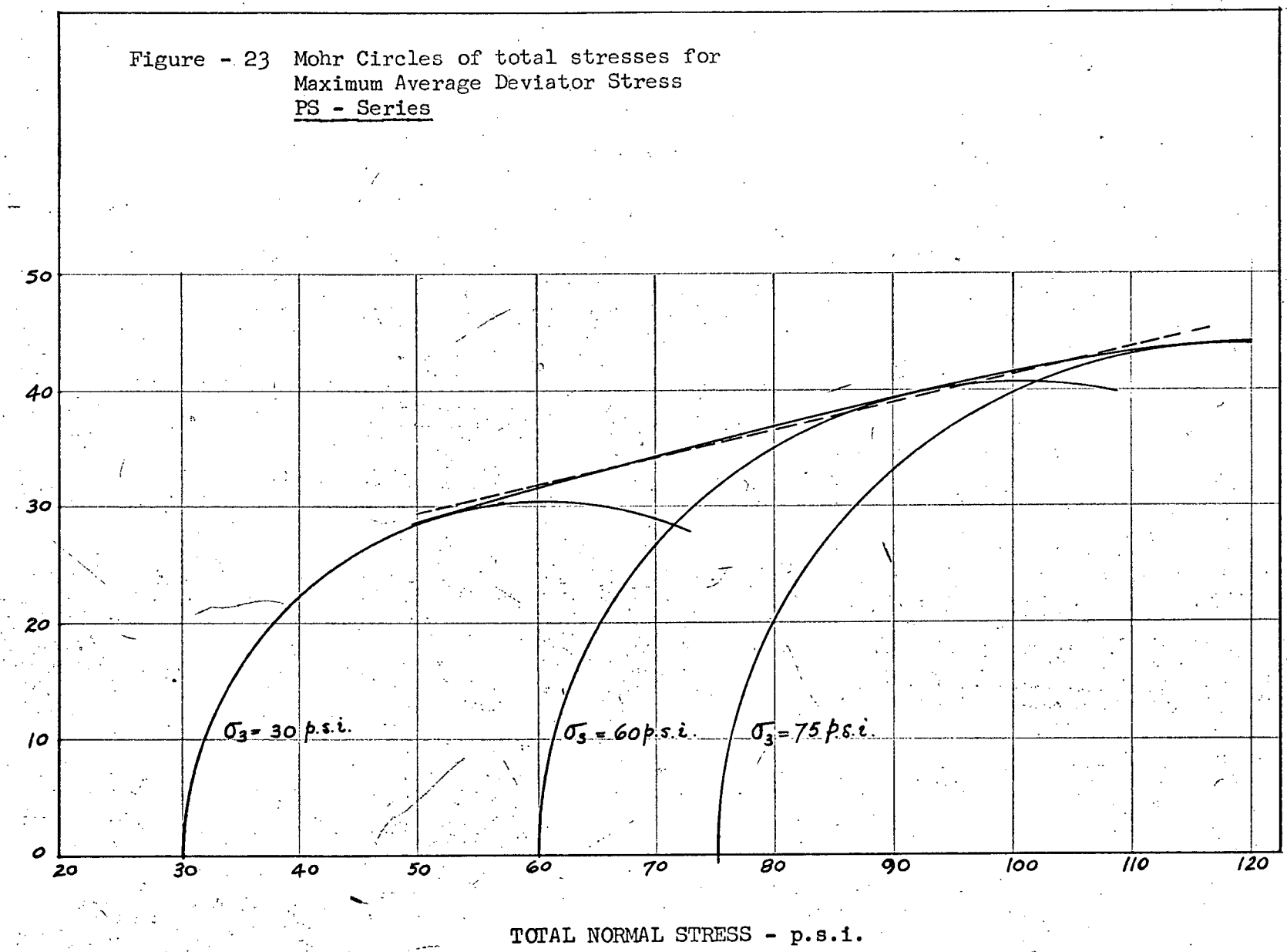

To follow Fig. 22

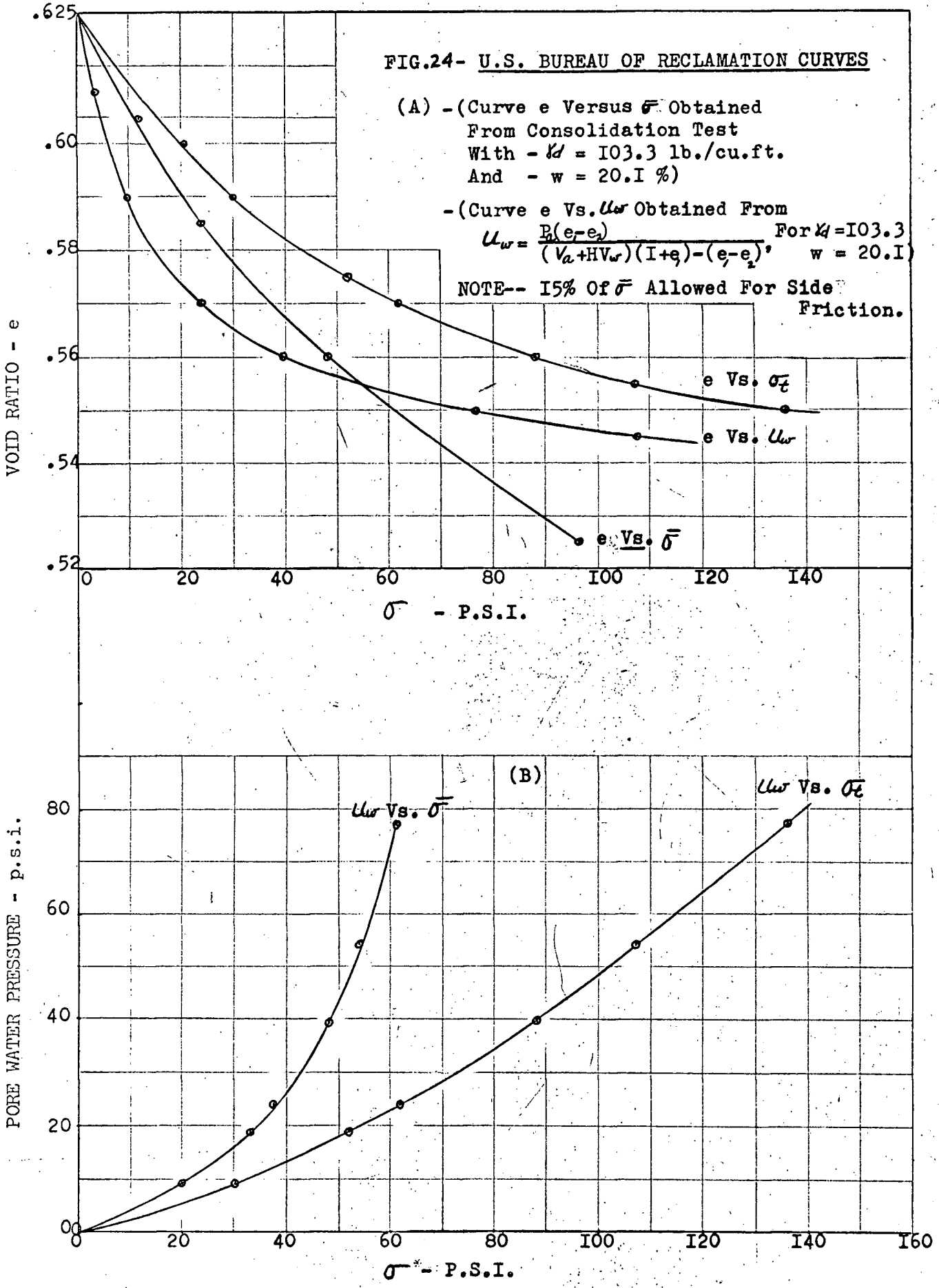
FIG.24- U.S. BUREAU OF RECLAMATION CURVES
(A) -(Curve e Versus σ̄ Obtained From Consolidation Test With - γd = 103.3 lb./cu.ft. And - w = 20.1 %)
-(Curve e Vs. uw Obtained From uw = Pa(e1-e2) / (Va+HVw)(1+e1)-(e1-e2), For γd=103.3 w = 20.1)
NOTE-- 15% Of σ̄ Allowed For Side Friction.
e Vs. σ̄t
e Vs. uw
e Vs. σ̄
VOID RATIO - e
.625
.60
.58
.56
.54
.52
0 20 40 60 80 100 120 140
σ̄ - P.S.I.
(B)
uw Vs. σ̄
uw Vs. σ̄t
PORE WATER PRESSURE - p.s.i.
80
60
40
20
0
0 20 40 60 80 100 120 140 160
σ̄ - P.S.I.

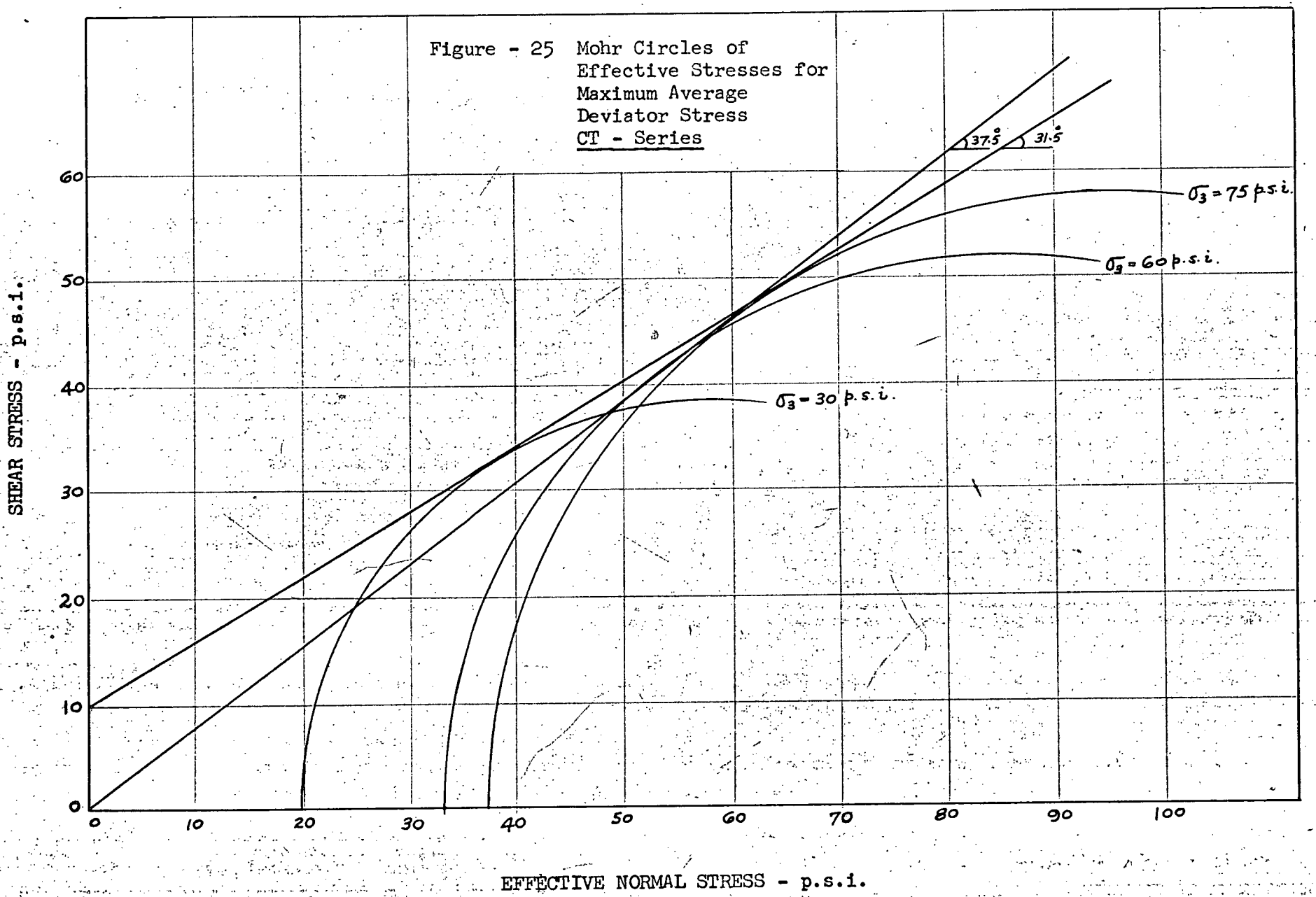

To follow Fig. 24

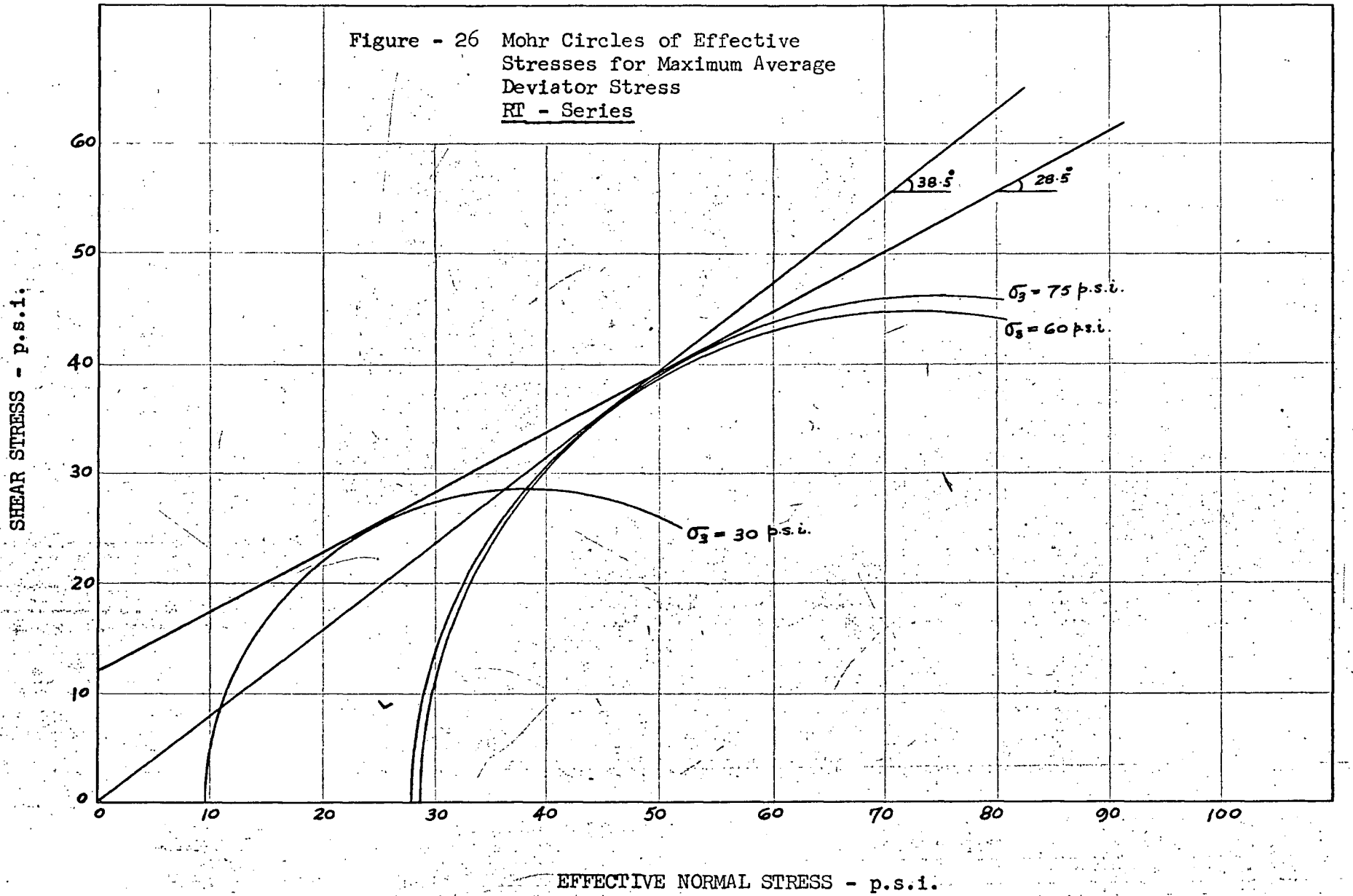

To follow Fig. 25

Figure - 27 Mohr Circles of Effective Stresses for Maximum Average Deviator Stress
PS - Series

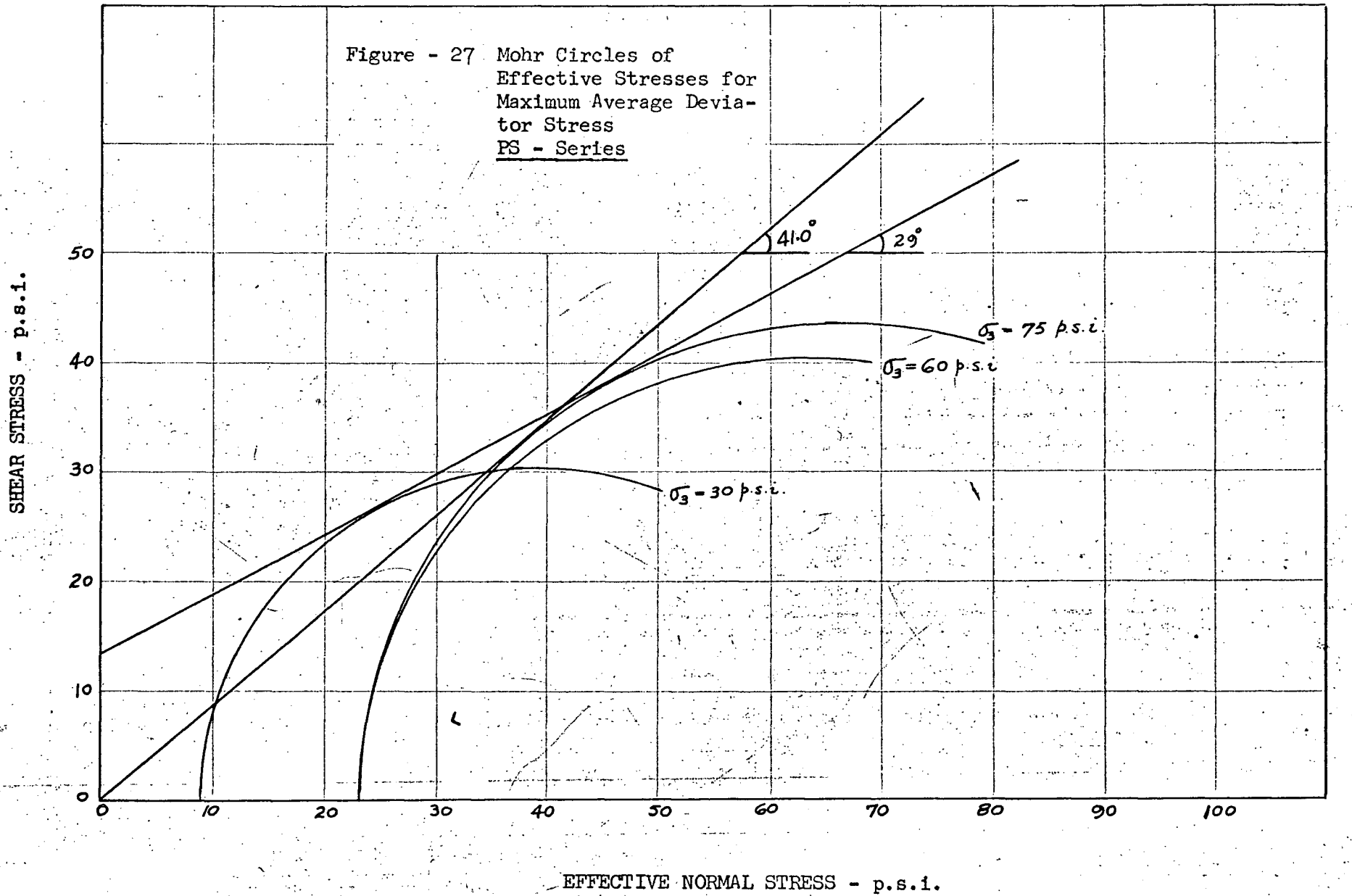

To follow Fig. 26

Figure - 28 Vector Curves
CT - Series

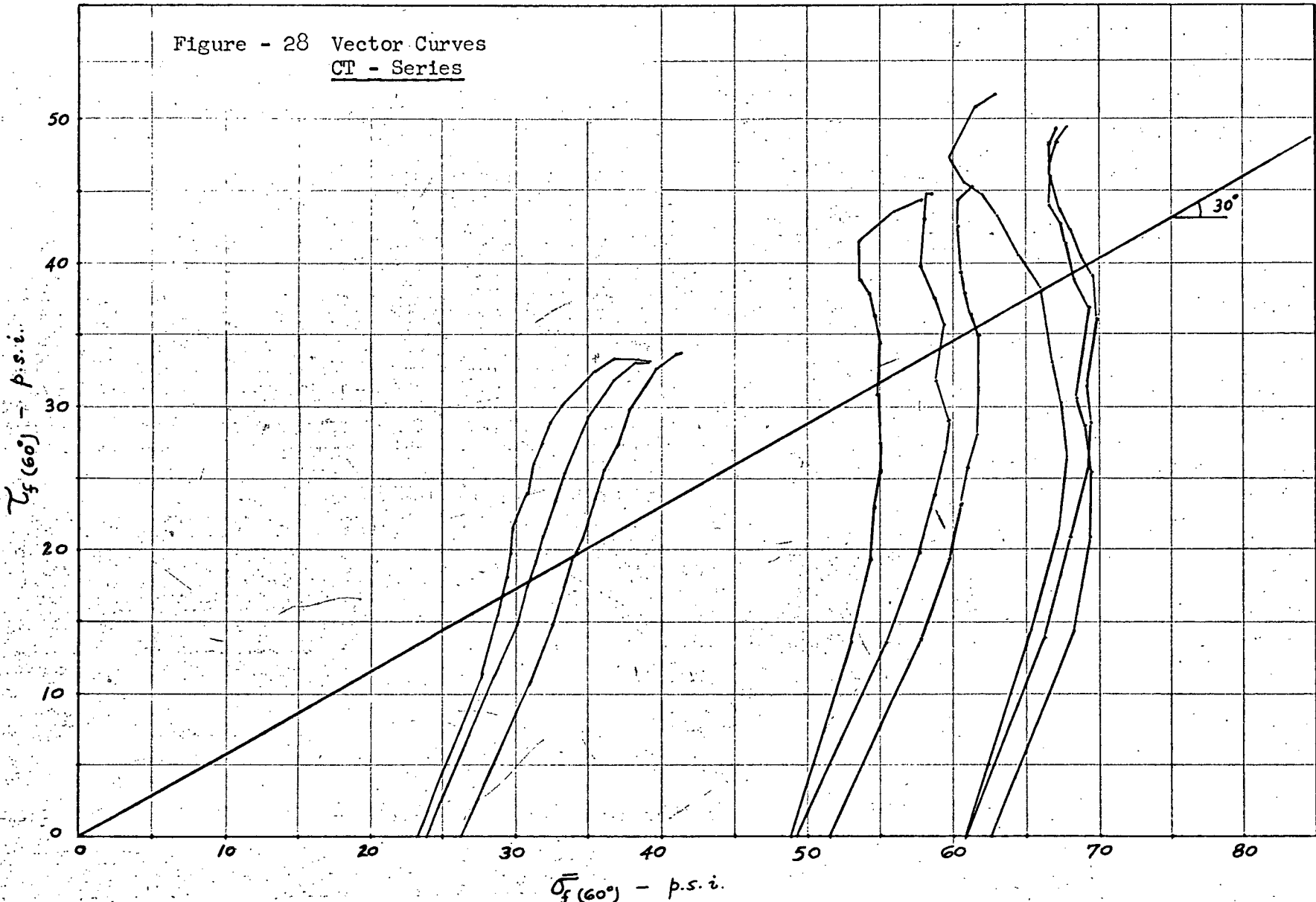

To follow Fig. 27.

Figure - 29 Vector Curves
RT - Series

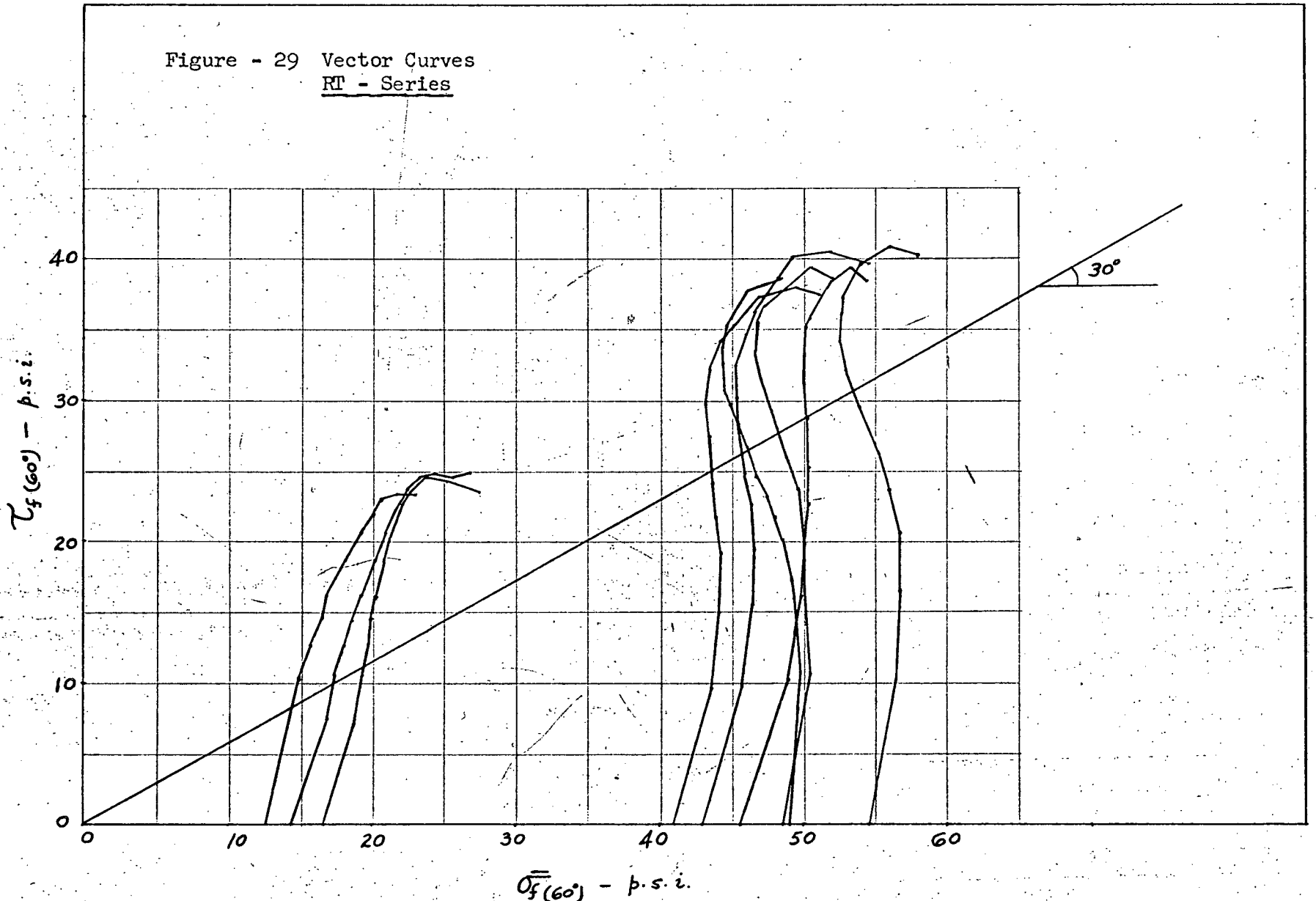

To follow Fig. 28

Figure - 30 Vector Curves
PS - Series

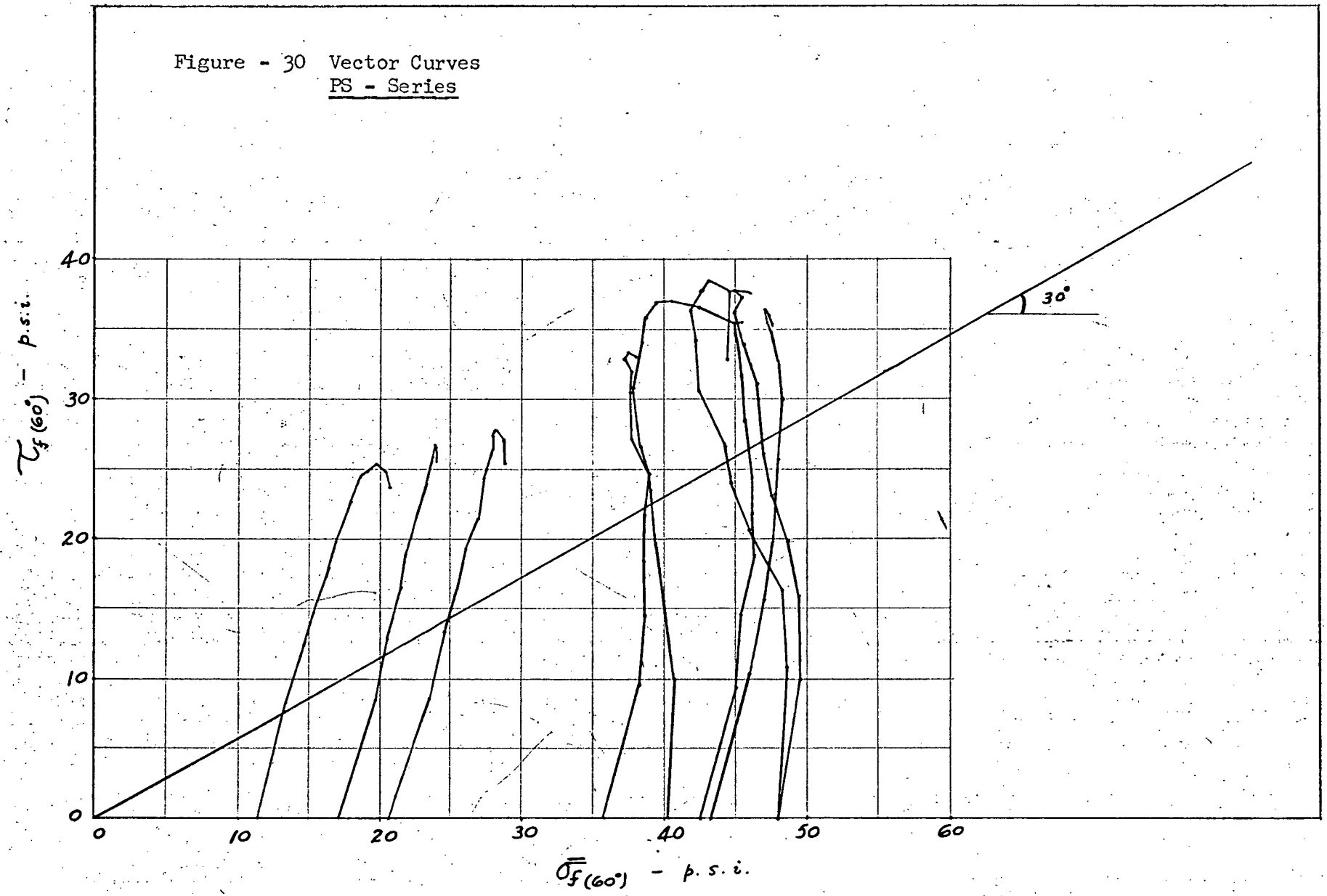

To follow Fig. 29

FIG.31 - TRANSDUCER CALBRATION CURVES

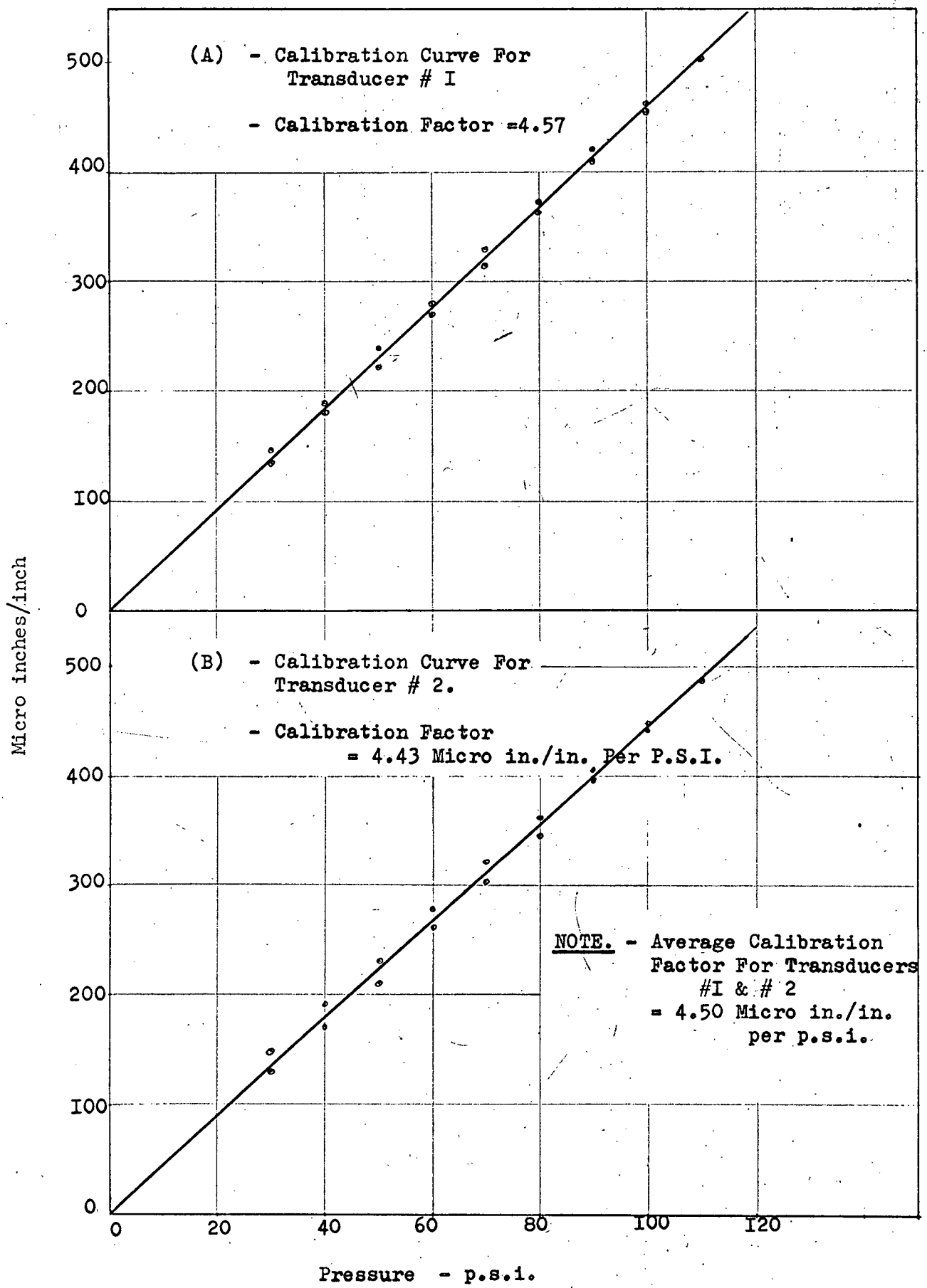

VI. DISCUSSION

A. Discussion of Testing Procedure

The effects of small random errors in individual tests were minimized by using, in each case, the average results of three identical tests. This discussion is therefore limited to sources of error inherent in the procedure.

The method mentioned under sample preparation and compaction procedure is believed to have eliminated or reduced error to a minimum, at least to within tolerable limits. The procedure, used in preparation of the sample and storage of the soil in gallon jars kept in the humid room, made it possible to do a test at a moments notice. Furthermore, for all 27 tests, the water content was quite close to 20.0%[1] ($\pm$ .5%). It was attempted to compact all specimens as nearly as possible to the same dry unit weight of about 103.0 lb/cu.ft.[2] The average water content, average dry unit weight and average degree of saturation are given in Table II.

The specimen volume changes were not measured during the triaxial tests; and in deducing cross-sectional areas for the computation of the deviator stress the volume changes were assumed to be negligible. In this case, since the compacted specimens were only partly saturated, there would definitely be some volume change which would put the deviator stress (calculated neglecting volume change) in error. However, this bold decision to neglect volume changes was taken after a careful study of the scope of this investigation and the equipment available.

---

(1) Optimum water content.

(2) Dry Unit weight obtained in Harvard Miniature Compaction.

The following were the two considerations upon which the author based his decision:

(1) Air voids in a specimen compacted to a dry unit weight of about 103.0 lbs./cu.ft. at a water content of 20.0% would occupy about 5½% of the total volume. Thus, the maximum change in volume, under undrained conditions (as in this case), would be at most, only 5½%. The actual amount of volume involved for 5½% volume change would range from about 3½ cu.cm. (for cylindrical specimens) to about 10 cu.cm. (for rectangular specimens). With the existing triaxial chamber and the volumeter available, it would not have been possible to measure accurately such small volume changes as these.

(2) Moreover, it was not deemed necessary to measure volume changes since the main purpose of this investigation was to study the relative difference in the shear characteristics obtained by three different types of tests - cylindrical triaxials, rectangular triaxials and plane strain. Thus, even though the deviator stress for a particular type of test might be in error by as much as about 5% (for 5½% volume change), the relative values of deviator stress for all three types of tests would not be affected by the fact that the volume changes were neglected.

To minimize the number of variables it was attempted to perform all tests under similar conditions. Unfortunately, the rate of axial strain used in testing cylindrical specimens (.27% strain per minute,) was different from the axial strain rate of .23% strain per minute used in testing rectangular specimens. The rate of vertical travel of the motor drive used

in all tests was approximately constant, but the original height of the rectangular specimen (3 in.) was different from that of the cylindrical specimen (2.816 in.) thus causing the axial strain rates to differ as described above. This is a possible source of error. However, the author believes that since this difference in axial strain rates was quite small it could not cause any serious error.

As described in the 'Testing Procedure", it was attempted to dry off any excess water around the porous stone prior to the testing phase of an experiment. Since there was no positive way of ensuring that the amount of water on the contact plane between the porous stone and the specimen was the same in all the tests, the author feels that this was one of the major sources of error in the experiments. For example, excess water on that contact plane would produce excessively high pore pressure readings during the test period. It would not affect only the parameter B but also the parameter A_f. The detailed discussion of the results with this factor in mind will be given later. Moreover, it is explained in reference (6) that "Porous stone end plates (except fine ceramic disks) were never satisfactory" for pore pressure measurements. Thus, the possibility that the pore pressures measured might not be 100 per cent correct should be recognized.

In case of plane strain tests, as described in the 'Testing Procedure", the length of the plane strain frame was adjusted, before assembling the triaxial chamber, in such a way as to bring the plane strain plates into contact with the soil specimen. During the period of time when confining pressure was being applied, there would be some decrease in volume of the

partly saturated specimen and consequently the sides of the specimen would not be in contact with the plane strain plates anymore. Thus it is believed that the plane strain condition was achieved only in the later part of the test after such time as the plates were, once again, in contact with the specimen. However, negative strains during the isotropic stress phase would be exactly reversed during the deviatoric stressing, so that overall strain in the direction normal to the intermediate principal plane would be zero.

It was explained before under "Equipment and Testing Procedure", that teflon (an almost frictionless material having a co-efficient of friction of 0.05) was used as the lining material for the plane strain plates. It was therefore possible to get almost uniform plane strain condition with very little restraint in the direction normal to the minor principal plane.

B. Discussion of Results

Each of the three series (CT, RT and PS) consisted of nine experiments, with three identical tests performed at each of the cell pressures, 30, 60 and 75 psi. The results of each set of three identical tests were averaged, so that each series finally has three sets of results, each being the average of three tests. The following discussion refers, in general, to these averaged results unless otherwise specified.

(i) Stress-strain curves - In figures 15 - 17 are plotted the average stress versus strain curves. For the CT and RT series of tests, the stress-strain curves are gradually curved, reaching a maximum deviator stress at strains of 20%, reflecting a plastic flow type failure. In the case of PS tests, the stress-strain curves are also gradually curved but reach

a maximum deviator stress at strains as low as about 10%, suggesting a shear plane type of failure. No failure planes were observed, however. The strains required to develop maximum deviator stress seems to be independent of the cell pressure. Hence it can be concluded that the strain required to develop maximum deviator stress under plane strain condition is about 50%[3] of that required to develop maximum deviator stress in the case of either RT or CT type of tests.

(ii) M_{50} - The secant modulus of deformation M50 (corresponding to 50% of the maximum deviator stress) is plotted in Fig. 19. This modulus increases with increasing cell pressure (σ_3). The total range of M_{50} in these tests was between about 1550 and 2900 lb/sq. in. Fig. 19 does not show a consistent pattern, although a general trend is established. It has been pointed out in reference (5) that 'The major cause of these irregularities in M_{50} may be the dependence of the shape of the initial portion of stress-strain curves upon the time elapsed between the compaction of a specimen and the start of the triaxial test". The elapsed time ranged from 30 minutes to 60 minutes in most of the tests.

(iii) Intermediate principal stress (σ_2) - In Figs. 15 - 17 are plotted the average ($\sigma_2 - \sigma_3$) versus axial strain curves for plane strain tests. For the first 1% strain in Fig. 15, for cell pressure of 30 psi, and about first 2.5% strain for cell pressures of 60 psi and 75 psi (Figs. 16, 17) the value of $\sigma_2 - \sigma_3$ is almost equal to zero, indicating that σ_2 is

---

(3) Since, as explained before, the plane strain condition was probably not achieved in the initial stages of axial loading, this figure may be lower than 50% for a 100% plane strain condition.

almost equal to σ_3. Hence no plane strain condition was achieved during those initial stages of the tests.(4) In the later part of the test, however, $\sigma_2 - \sigma_3$ increases at the rate of about 50% of $\sigma_1 - \sigma_3$ with strain, indicating that σ_2 is about equal to $\frac{\sigma_1 + \sigma_3}{2}$, or, that $\bar{\sigma}_2$ is equal to about $\frac{\bar{\sigma}_1 + \bar{\sigma}_3}{2}$. As explained before, for plane strain condition $\bar{\sigma}_2$ can be expected to be equal to $\mu(\bar{\sigma}_1 + \bar{\sigma}_3)$. It is, therfore, concluded that μ (Poisson's ratio) for the soil used in this investigation is equal to about 0.5.

(iv) Pore Pressure Parameters

Parameter B - In Fig.18 is plotted the parameter B as a function of cell pressure. Results are inconsistent. It is believed that the major cause of these irregularities in the values of B is the failure in achieving the same amount of water on the contact plane between the porous stone and the soil specimen in every test. As described in "Discussion of Testing Procedure" different amounts of water on this contact plane will lead to different pore pressure readings, for similar cell pressures (σ_3); and different pore pressure readings will give different values of B, hence the inconsistent results as shown in Fig.18.

In the PS series, the plane strain condition was not achieved while the all-round (cell) pressure was being applied. Thus the author was unable to study the effect of plane strain on the parameter B.

---

(4) This confirms the explanation given in the last part of "Discussion of testing procedure", page (29).

Parameter A_f - The value of parameter A_f changes throughout the axial loading phase of the tests. The overall average value, from the start of the axial loading to the load at failure, is the one that has the most practical significance. Thus it became important to decide at what point on the stress-strain curve failure has occured. In figure 20 are plotted curves of the pore pressure parameter A_f versus cell pressure for all three types of tests. The criteria of failure used are as follow:

(1) The maximum deviator stress that the specimen can stand during the test.

(2) The maximum effective principal stress ratio $\bar{\sigma}_1/\bar{\sigma}_3$.

(3) A limiting axial strain of 10% - 10% axial strain to represent failure was selected because of the fact that maximum deviator stress for most of the plane strain tests occured at this 10% strain.

Though the curves for the PS series in Fig.20, for all three criteria of failure, lie above those for the CT or the RT series of tests (indicating comparatively higher values of A_f for the PS tests), only tentative conclusions can be drawn at this stage, because of the following two errors in the testing procedure:

(1) The plane strain condition did not exist in the early stages of the tests and thus the curves do not show the full effect of plane strain on A_f.

(2) As explained before, A_f is a product of A and B;[5] and the value of B which applies during deviatoric stressing is different from that

---

(5) See equations (6) and (7).

which is applicable during application of cell pressure. However, as pointed out in reference (6), the B-value which is applicable during actual stressing is very much dependent on the B-value obtained during the isotropic stress phase. The value of A_f, therefore is affected by the B-value obtained during application of all-round pressure, which, as shown in Fig.18, is quite inconsistent.

(v) Mohr Circles (total stresses)

In Figs. 21 - 23 are plotted the Mohr circles (in terms of total stresses) for maximum deviator stress. As is apparent from the envelopes drawn in Figs.21 - 23, at small cell pressures the strength increases rapidly with increasing cell pressure but at large cell pressures the strength increases very little with increasing cell pressure. It is believed that when cell pressures are large enough almost all the pore air goes into solution in the pore water and the specimen becomes practically saturated. Any increase in confining pressure, then, goes directly to increase the pore pressure by the full amount and the effective confining pressure, thus, does not increase. Since the strength depends upon the effective confining pressure and not upon the total confining pressure, little or no increase in strength is achieved by increasing the cell pressure once the specimen becomes nearly saturated. The so-called U.S. Bureau of Reclamation curves plotted in Fig.24 show this effect of large cell pressures on the degree of saturation of the specimens quite clearly. It is apparent from Fig.24B, that after the value of σ_t (total confining pressure) is larger than about 90 psi, the pore pressure increases almost by the full amount of increase in σ_t and the value of $\bar{\sigma}$ (effective confining pressure) stays almost constant.

(vi) Mohr Circles (effective stresses)

In Figs.25 - 27 are plotted the Mohr circles (in terms of effective stresses) for maximum deviator stress. The strength envelopes drawn to touch the smallest and the largest circles show the following results:

TABLE IV

STRENGTH PARAMETERS

Series	c'	ϕ'
CT	10	31.5°
RT	12	28.5°
PS	13.5	29.0°

At low confining pressures, the compacted specimens are believed to have behaved in a manner similar to that for overly consolidated soils. Thus envelopes are also drawn to pass through the origin and to touch the largest circle. The results are given in Table V as follows:

TABLE V

ϕ' - VALUES FOR $C' = 0$

Series	ϕ'
CT	37.5°
RT	38.5°
PS	41.0°

These values would be applicable at high stresses assuming that there was no cohesion at 75 psi chamber pressure.

If Mohr circles were drawn for deviator stress at 10%[6] axial strain, the ϕ'-values for the CT and the RT series would be much smaller than the corresponding values in Table IV and Table V. Thus it can be concluded that ϕ'-values obtained in plane strain tests are definitely higher than that for the RT series.

(vii) Vector Curves

In Figs. 28 - 30 are plotted the vector curves for stresses on the failure plane for each individual test. They were computed on the assumption that the failure plane is inclined at 60^{o} to the major principal plane, assuming an internal angle of friction of 30 degrees. The end points of all the vector curves lie well above the 30-degree line.

---

(6) 10% axial strain is one of the criteria of failure previously used.

VII. SUMMARY OF CONCLUSIONS

Based on the data and discussions presented in this thesis, it may be concluded that:

(1) For compacted clayey soils, the strain required to develop maximum deviator stress under plane strain condition is less than about 50% of that required in the case of a corresponding conventional triaxial test.

(2) The value of intermediate principal stress under plane strain condition is half way between the major and minor principal stresses.

(3) The Poisson's ratio for silty clay such as the one used in this investigation is about 0.5.

(4) The value of Pore Pressure parameter A_f at failure, in plane strain is definitely higher than that for the corresponding conventional triaxial test.

(5) The values of the strength parameters (c', ϕ') in plane strain are higher than those for the corresponding conventional triaxial tests.

In the above remarks, "Corresponding" means a test run under the same conditions (cell pressure, rate of strain, etc.) on a specimen of the same shape.

VIII. RECOMMENDATIONS

Further investigations are needed on every phase of the work reported in this thesis. The time and testing were limited, resulting in data that need verification by investigators in future.

The following are two changes in the equipment, which could improve the quality of the results to a great extent:

(1) Use of ceramic end plates instead of porous stones (as used in this investigation).

(2) Provision for adjusting the length of the plane strain frame after the application of cell pressure.

APPENDIX I

TEST RESULTS

TABLE NO. VI AS-MOULDED CONDITIONS

CYLINDRICAL TRIAXIAL SERIES				RECTANGULAR TRIAXIAL SERIES				PLANE STRAIN SERIES			
TEST NO.	WATER CONTENT %	DRY DENSITY lbs./cu.ft.	$S_{\%}$	TEST NO.	$W_{\%}$	γ_d lbs./cu.ft.	$S_{\%}$	TEST NO.	$W_{\%}$	γ_d lbs./cu.ft.	$S_{\%}$
1		102.2	84.5	10	20.25	103.2	86.3	19	20.08	104.7	89.3
2		102.3	84.8	11	20.35	103.5	87.2	20	19.90	103.8	87.1
3		102.3	85.2	12	20.33	103.3	86.5	21	19.95	103.9	87.3
Ave.	20.02	102.3	84.8	Ave.	20.31	103.3	86.7	Ave.	19.98	104.1	87.9
4		102.8	87.4	13		104.2	89.5	22	20.1	102.9	85.0
5		103.5	88.2	14		104.0	88.7	23	20.1	103.8	87.0
6		103.5	88.2	15		104.2	89.5	24	19.8	104.6	89.0
Ave.	20.30	103.3	87.9	Ave.	20.2	104.1	89.2	Ave.	20.0	103.8	87.0
7	20.05	102.8	85.3	16	20.5	104.0	89.0	25	20.08	104.5	88.4
8	20.00	102.2	85.2	17	20.3	103.5	87.7	26	19.95	104.8	89.0
9		102.8	85.3	18	20.4	104.5	90.0	27	19.70	104.5	88.4
Ave.	20.02	102.6	85.3	Ave.	20.3	104.0	88.9	Ave.	19.91	104.6	88.6
Overall Ave.	20.11	102.7	86.0	Overall Ave.	20.27	103.8	88.3	Overall Ave.	19.96	104.5	87.8

TABLE NO. VII PORE PRESSURE PARAMETER B

CYLINDRICAL TRIAXIAL SERIES				RECTANGULAR TRIAXIAL SERIES				PLANE STRAIN SERIES			
TEST NO.	σ_3 p.s.i.	u_o p.s.i.	B	TEST NO.	σ_3 p.s.i.	u_o p.s.i.	B	TEST NO.	σ_3 p.s.i.	u_o p.s.i.	B
1	30	7^-	.225	10	30	16^-	.525	19	30	19^-	.625
2	30	6.5^-	.208	11	30	13.5	.450	20	30	13.0	.433
3	30	4^-	.125	12	30	17.5	.582	21	30	9.5	.317
Ave.		5.5	.186	Ave.		15.6	.519	Ave.		13.8	.458
4	60	11^+	.187	13	60	19.0	.316	22	60	17.5	.292
5	60	8.5	.142	14	60	17.0	.283	23	60	17^-	.280
6	60	11^-	.179	15	60	14.5	.242	24	60	24^+	.405
Ave.		10.2	.169	Ave.		16.2	.270	Ave.		19.6	.326
7	75	12.5	.167	16	75	26.5	.354	25	75	35^-	.463
8	75	14^+	.190	17	75	20.5	.274	26	75	27.0	.360
9	75	14^+	.190	18	75	26.0	.347	27	75	27.0	.360
Ave.		13.7	.182	Ave.		24.4	.325	Ave.		29.5	.394

TABLE VIII PORE PRESSURE PARAMETER A_f

SERIES	TEST NO.	σ_3 p.s.i.	FOR MAX. DEVIATOR STRESS: ϵ %	$\sigma_1-\sigma_3$ p.s.i.	$u-u_o$ p.s.i.	A_f	TIME OF LOADING MIN.	M_{50} p.s.i.	FOR MAX. $\bar{\sigma}_1/\bar{\sigma}_3$: ϵ %	$\bar{\sigma}_1$ p.s.i.	$\bar{\sigma}_1/\bar{\sigma}_3$	$\bar{\sigma}_3$ p.s.i.	A_f	FOR 10% STRAIN: $\sigma_1-\sigma_3$ psi.	$u-u_o$ p.s.i.	A_f
CYLINDRICAL TRIAXIALS	1	30	17.8	76.8	5.7	.074	69		14.20	91.7	5.50	16.7	.087	68.0	8.4	.124
	2	30	17.8	76.3	4.7	.062	68		14.2	91.8	5.02	18.3	.075	66.1	5.5	.083
	3	30	17.8	77.8	4.8	.062	66		14.2	96.1	4.62	20.8	.073	67.6	5.5	.82
						.066		2400		93.2		18.6	.078	67.2	6.5	.096
	4	60	21.4	102.5	16.5	.162	79		17.8	131.6	4.28	30.8	.178	88.5	17.0	.192
	5	60	21.4	104.3	16.5	.158	75		21.4	139.3	3.98	35.0	.158	89.1	13.1	.147
	6	60	18.6	103.5	17.0	.166	76		21.4	135.8	4.25	32.0	.166	90.2	13.8	.153
						.162		2700		135.6		32.6	.167	89.3	14.6	.164
	7	75	21.4	114.5	23.2	.203	75		21.4	153.7	3.92	39.2	.203	100.2	20.6	.205
	8	75	21.4	113.5	22.3	.196	76		21.4	152.0	3.95	38.5	.196	98.8	19.8	.201
	9	75	21.4	119.5	27.7	.232	75		17.8	149.6	4.68	32.0	.244	104.4	21.1	.202
						.210		2900		151.8		36.6	.213	101.1	20.5	.202
RECTANGULAR TRIAXIALS	10	30	13.3	57.3	4.2	.074	59		10	65.6	7.29	9.0	.093	56.6	5.2	.092
	11	30	10.0	56.9	7.0	.123	42		8.7	63.6	7.07	9.0	.137	56.9	7.0	.123
	12	30	10.0	54.0	4.2	.078	45		7.3	57.9	7.94	7.3	.104	54.0	4.3	.080
						.092		1550		62.4		8.4	.111	55.8	5.5	.098
	13	60	16.7	88.0	13.7	.156	72		13.3	111.5	4.37	25.5	.180	81.0	16.3	.201
	14	60	16.7	88.0	16.5	.187	68		13.3	111.3	4.40	25.3	.206	81.6	18.0	.220
	15	60	16.7	91.0	15.5	.165	75		13.3	118.5	3.99	29.7	.178	82.7	15.8	.191
						.169		2300		113.8		26.9	.188	81.8	16.7	.204

TABLE VIII Continued

SERIES	TEST NO.	σ_3 p.s.i	FOR MAX. DEVIATOR STRESS					M_{50}	FOR MAX. $\bar{\sigma}_1/\bar{\sigma}_3$					FOR 10% STRAIN		
			ϵ %	$\sigma_1-\sigma_3$ p.s.i	$u-u_o$ p.s.i	A_f	TIME OF LOADING MIN.	p.s.i	ϵ %	$\bar{\sigma}_1$ p.s.i	$\bar{\sigma}_1/\bar{\sigma}_3$	$\bar{\sigma}_3$ p.s.i	A_f	$\sigma_1-\sigma_3$ p.s.i	$u-u_o$ p.s.i	A_f
PLANE STRAIN	16	75	16.7	90.7	20.7	.228	67		10.0	110.7	4.26	26.0	.249	84.7	22.5	.266
	17	75	16.7	94.5	22.0	.233	71		13.3	123.0	3.97	31.0	.255	86.0	23.2	.270
	18	75	16.7	93.8	20.7	.221	72		13.3	118.5	4.56	26.0	.249	87.0	23.8	.273
						.227		2450		117.4		27.7	.251	85.9	23.2	.270
	19	30	8.7	58.3	6.2	.108	38		6.0	60.9	13.55	4.5	.120	57.4	5.2	.091
	20	30	7.3	61.6	8.5	.138	30		7.3	70.1	8.25	8.5	.138	59.0	7.8	.132
	21	30	8.7	64.0	8.2	.129	36		8.7	70.25	6.25	12.2	.129	62.4	7.3	.117
						.125		2200		67.1		8.4	.129	59.6	6.8	.113
	22	60	10.0	81.6	18.0	.228	48		10.0	106.1	4.34	24.5	.228	81.4	18.0	.221
	23	60	10.0	83.8	17.0	.203	44		10.0	110.0	4.20	26.2	.203	83.8	17.0	.203
	24	60	10.0	76.8	17.5	.221	41		10.0	95.0	5.22	18.2	.221	76.8	17.6	.229
						.217		2350		103.7		23.0	.217	80.7	17.5	.218
	25	75	10.0	85.5	21.0	.246	45		8.7	103.2	5.67	18.2	.259	85.5	21.0	.245
	26	75	10.0	88.5	27.0	.305	44		10.0	109.5	5.22	21.0	.305	88.5	27.0	.305
	27	75	10.0	87.2	25.0	.287	41		10.0	110.2	4.79	23.0	.287	87.2	25.0	.287
						.279		2600		107.6		20.7	.284	87.1	24.3	.279

Figure-32. Cylindrical Triaxial Series
Stress - Strain Curves
Cell Pressure = 30 lbs/sq. in.^{2}

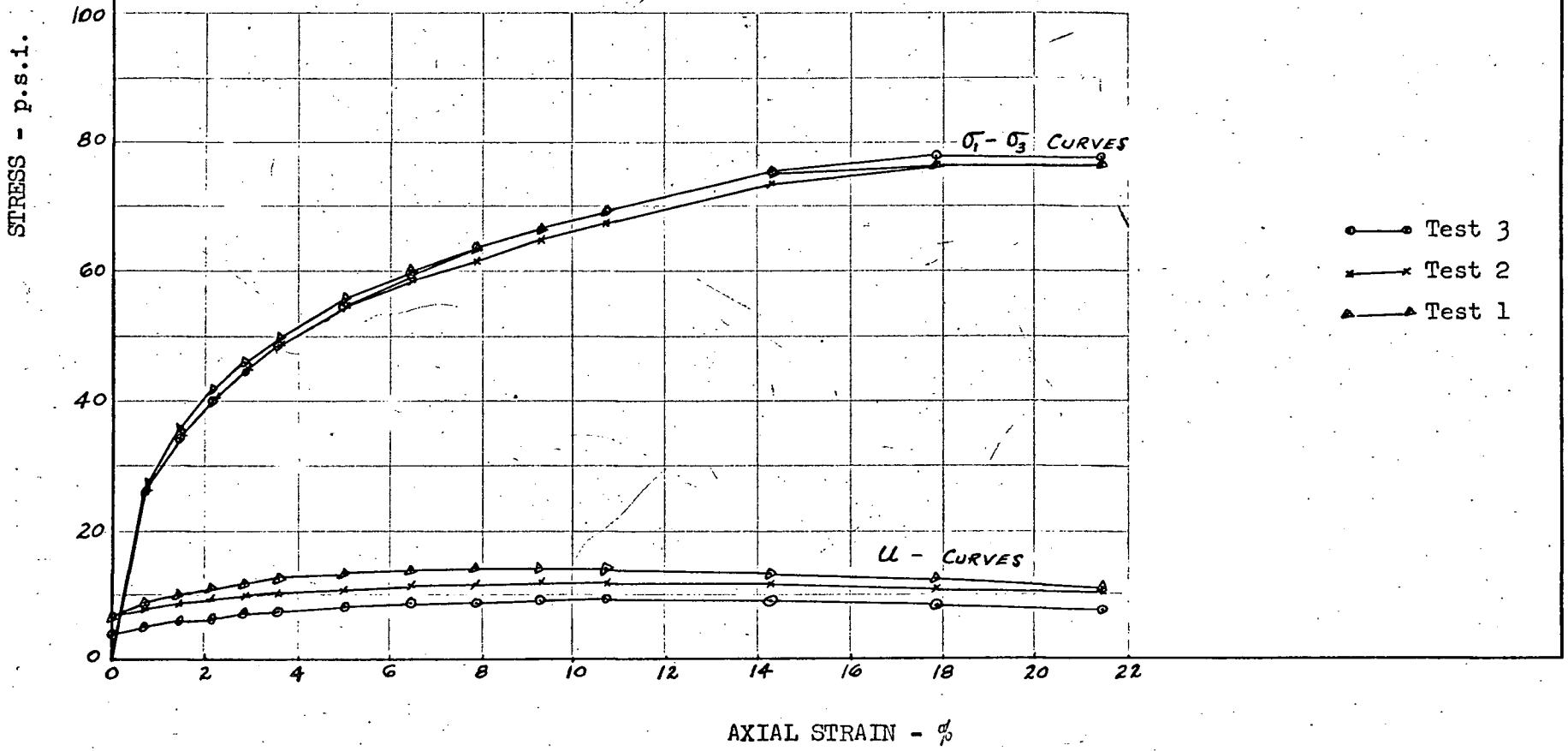

To follow page 41

Figure - 33 Cylindrical Triaxial Series
Stress-Strain Curves
Cell pressure = 60 lbs./sq. in.^{2}

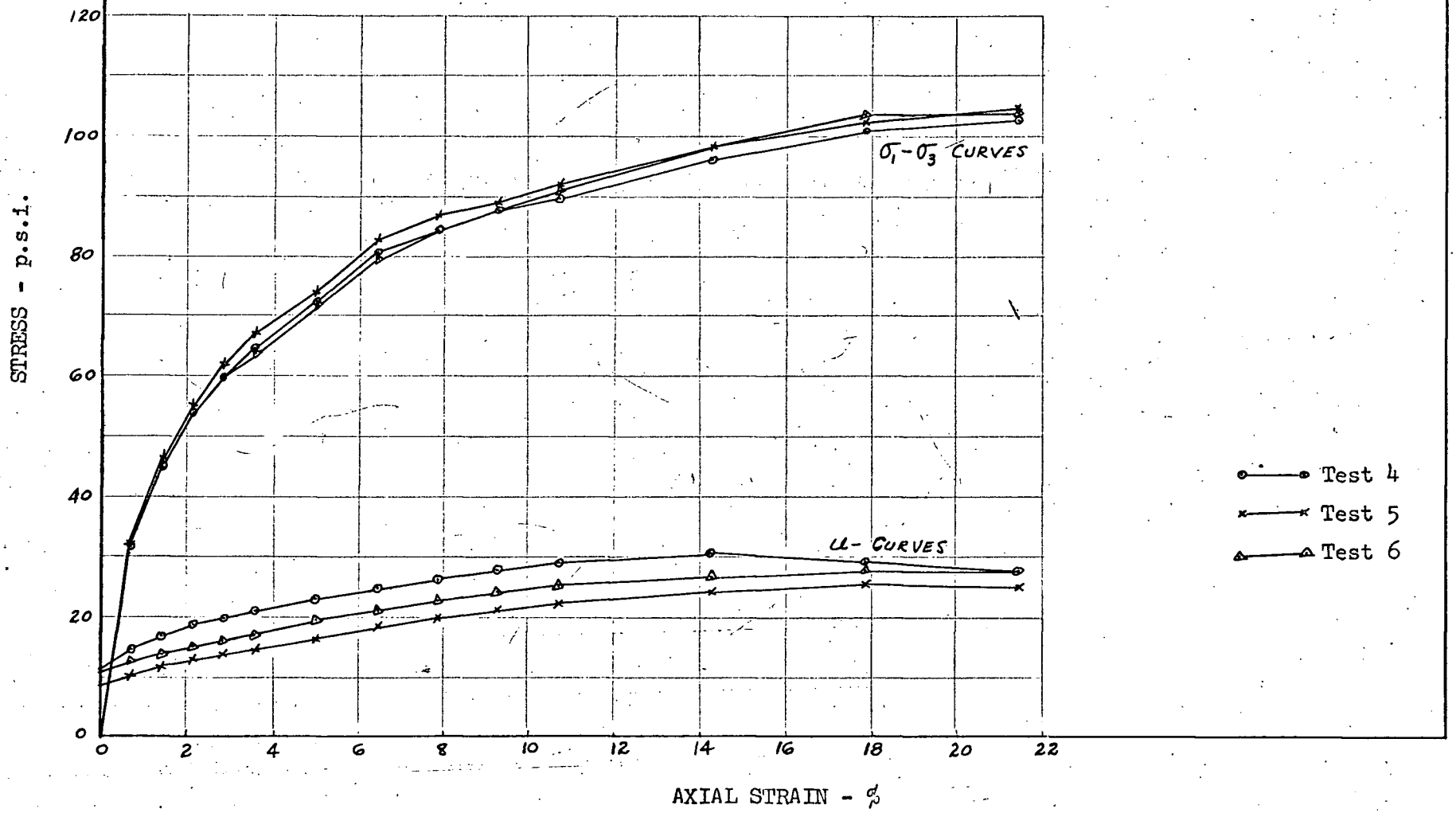

To follow Fig. 32

Figure - 34 Cylindrical Triaxial Series
Stress-Strain Curves
Cell pressure = 75 lbs./sq. in.^{2}

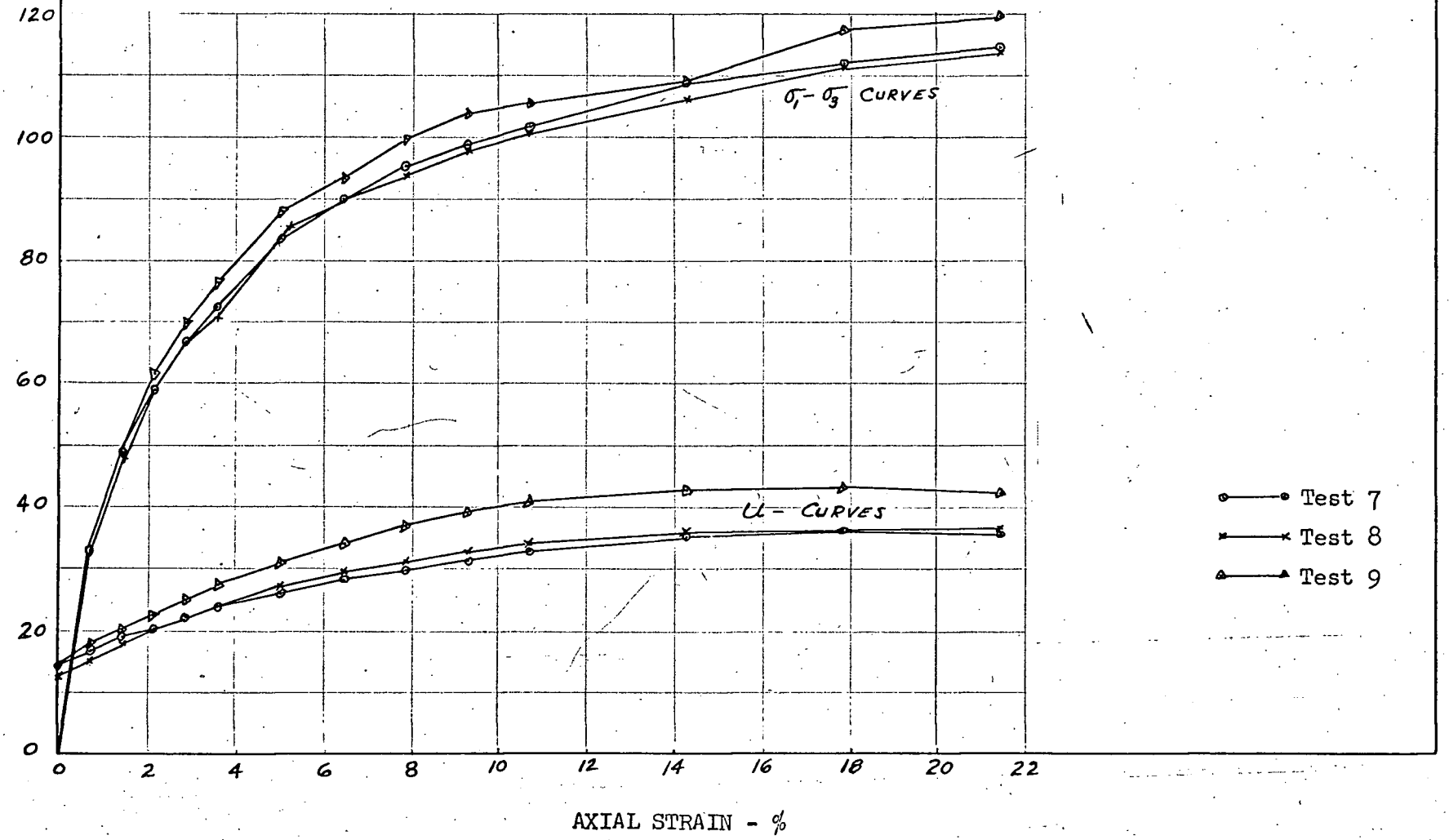

To follow Fig. 33

Figure - 35 Rectangular Triaxial Series
Stress-Strain Curves
Cell pressure = 30 lbs/sq. in.^{2}

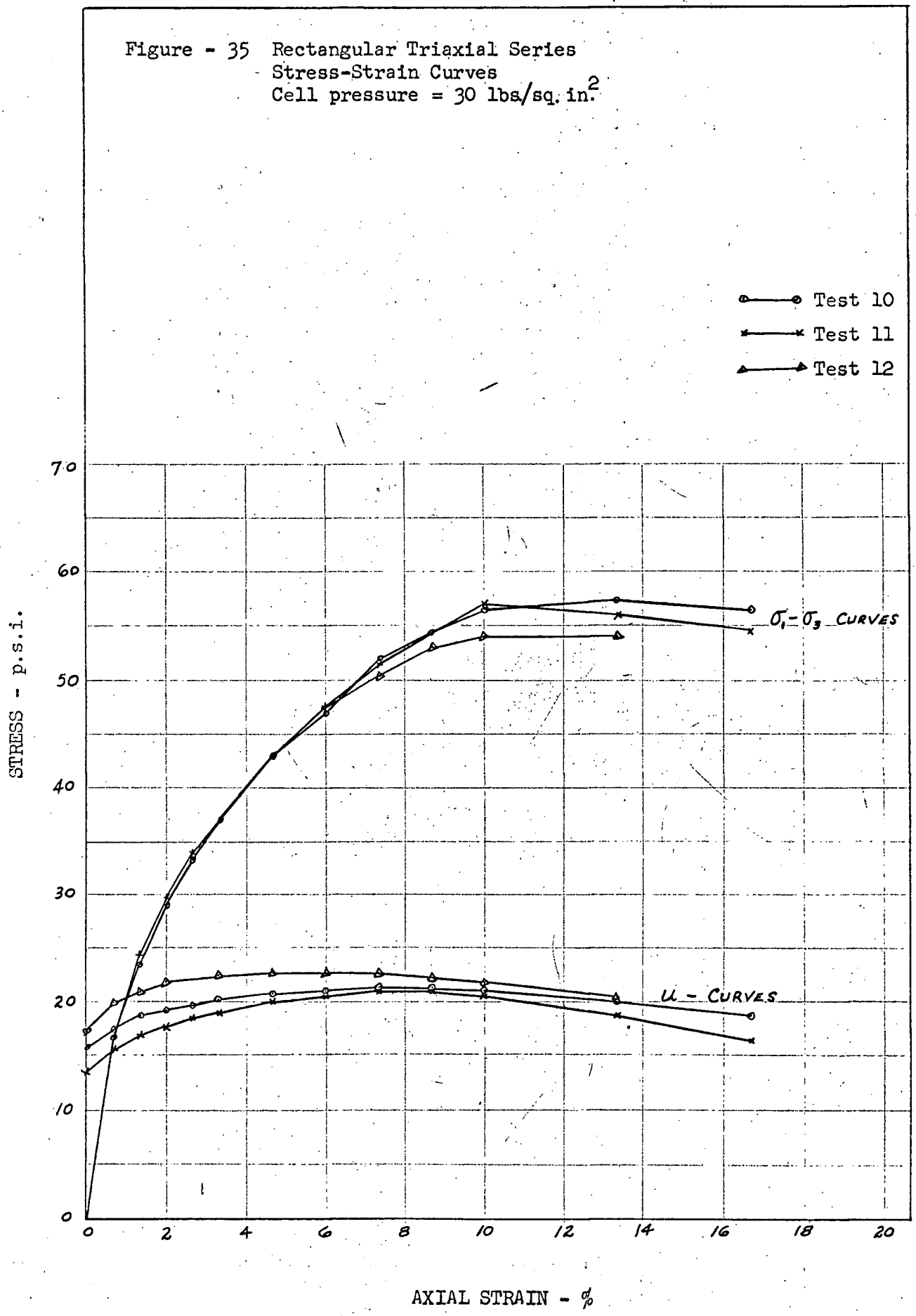

Figure - 36 Rectangular Triaxial Series
Stress-Strain Curves
Cell pressure = 60 psi.

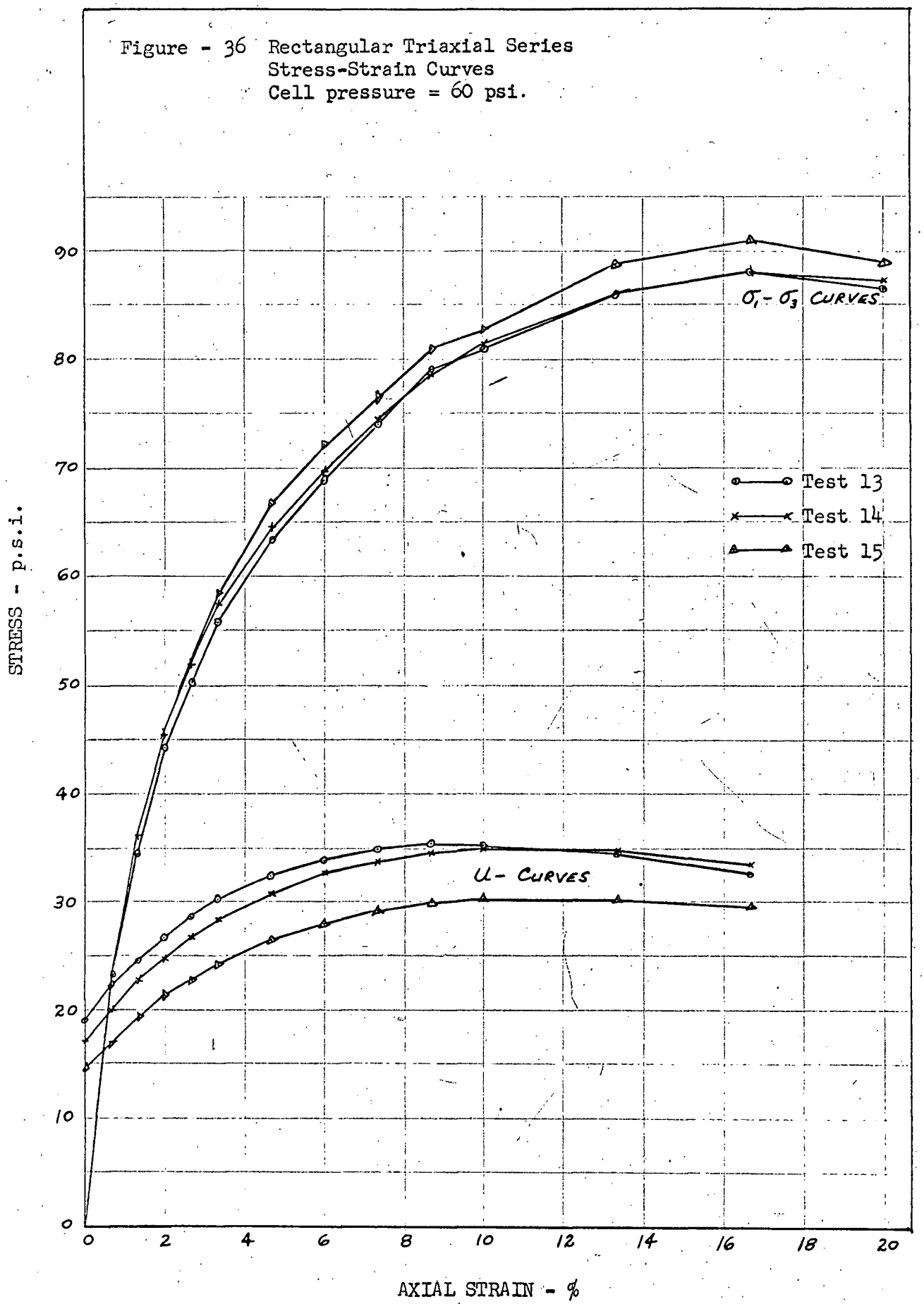

Figure - 37 Rectangular Triaxial Series
Stress-Strain Curves
Cell pressure = 75 lbs./sq. in.^{2}

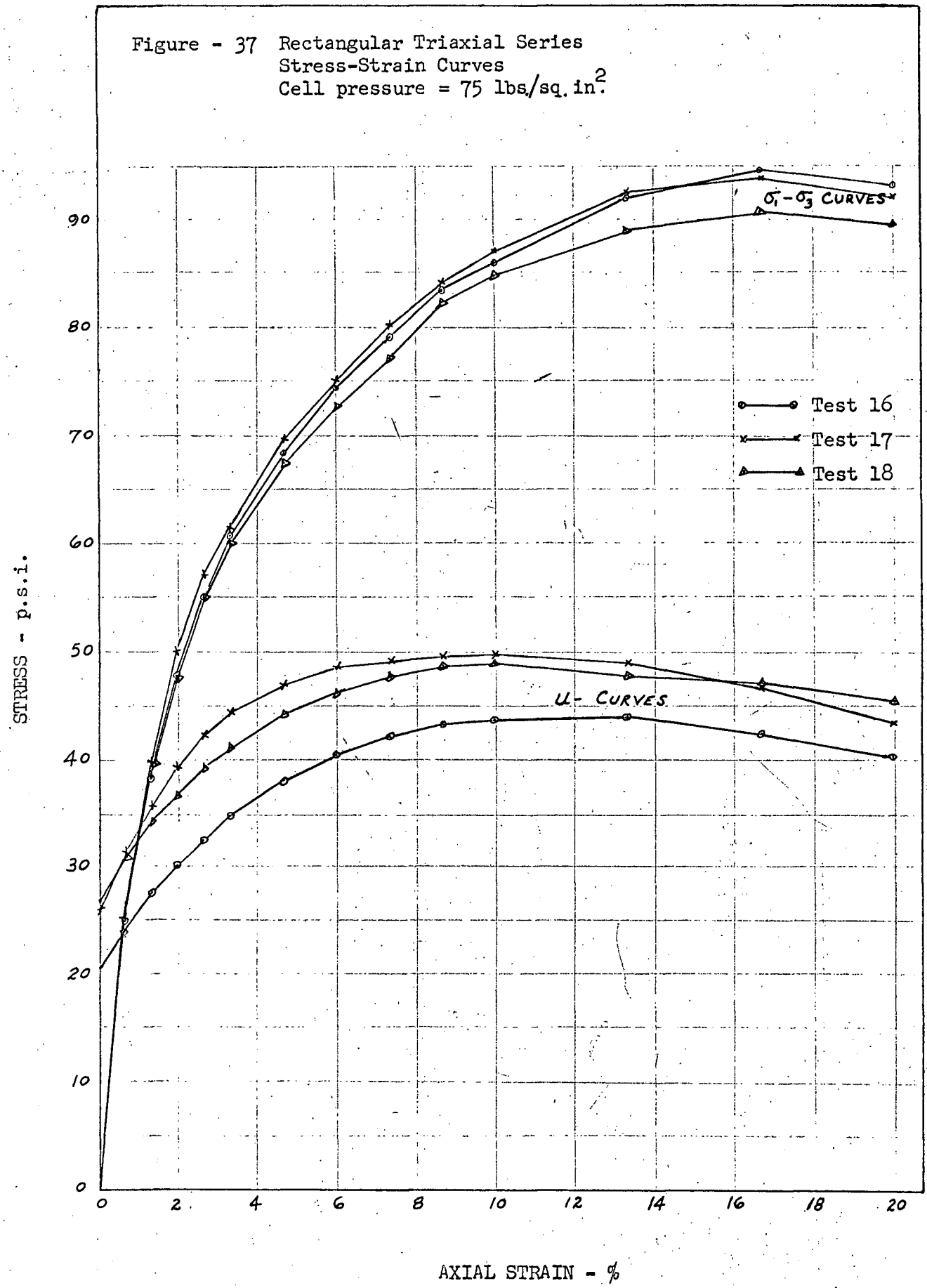

Figure - 38 Plane Strain Series
Stress-Strain Curves
Cell pressure = 30 lbs./sq. in.^{2}

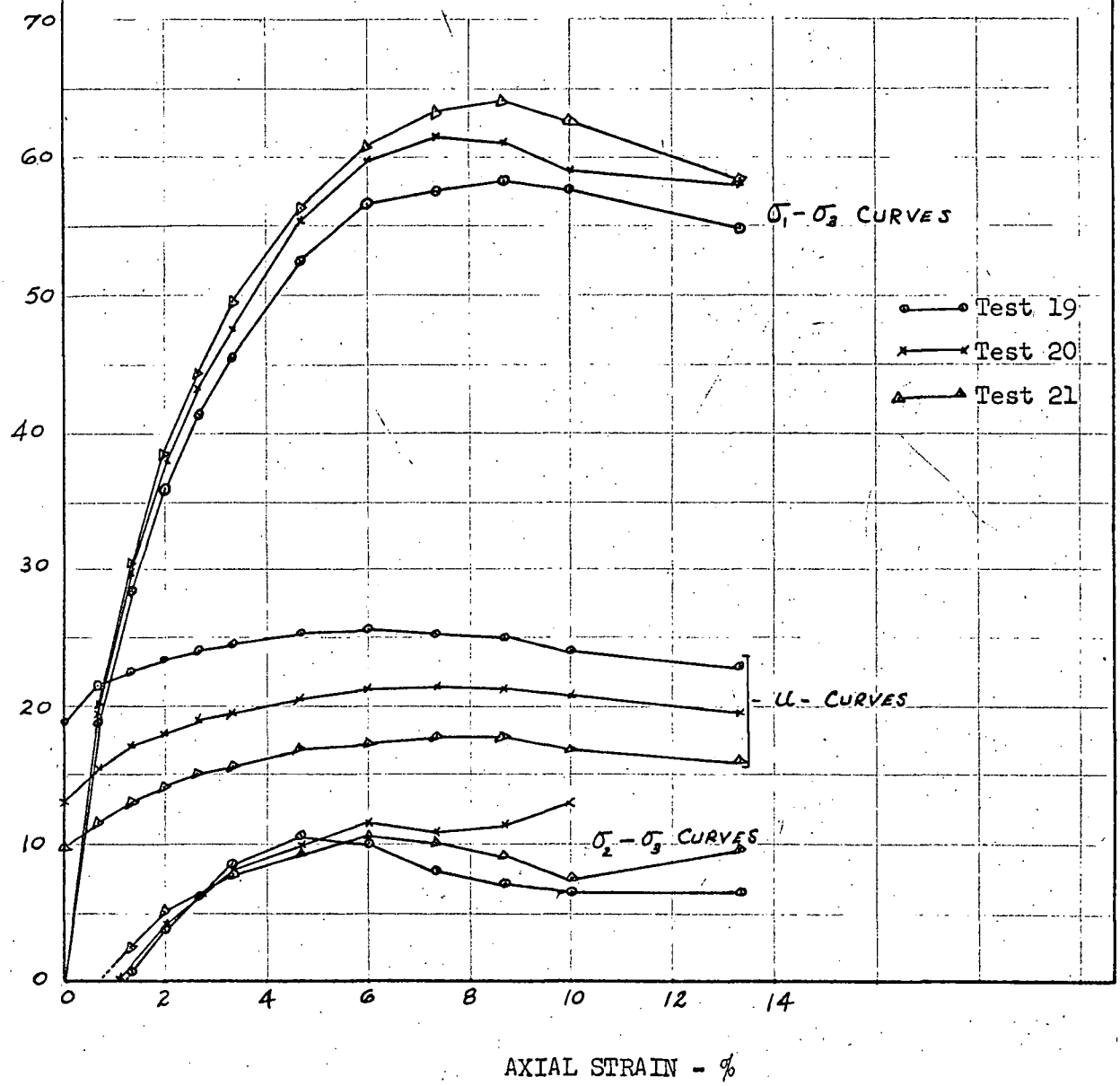

Figure - 39 Plane Strain Series
Stress-Strain Curves
Cell pressure = 60 lbs./sq. in.^{2}

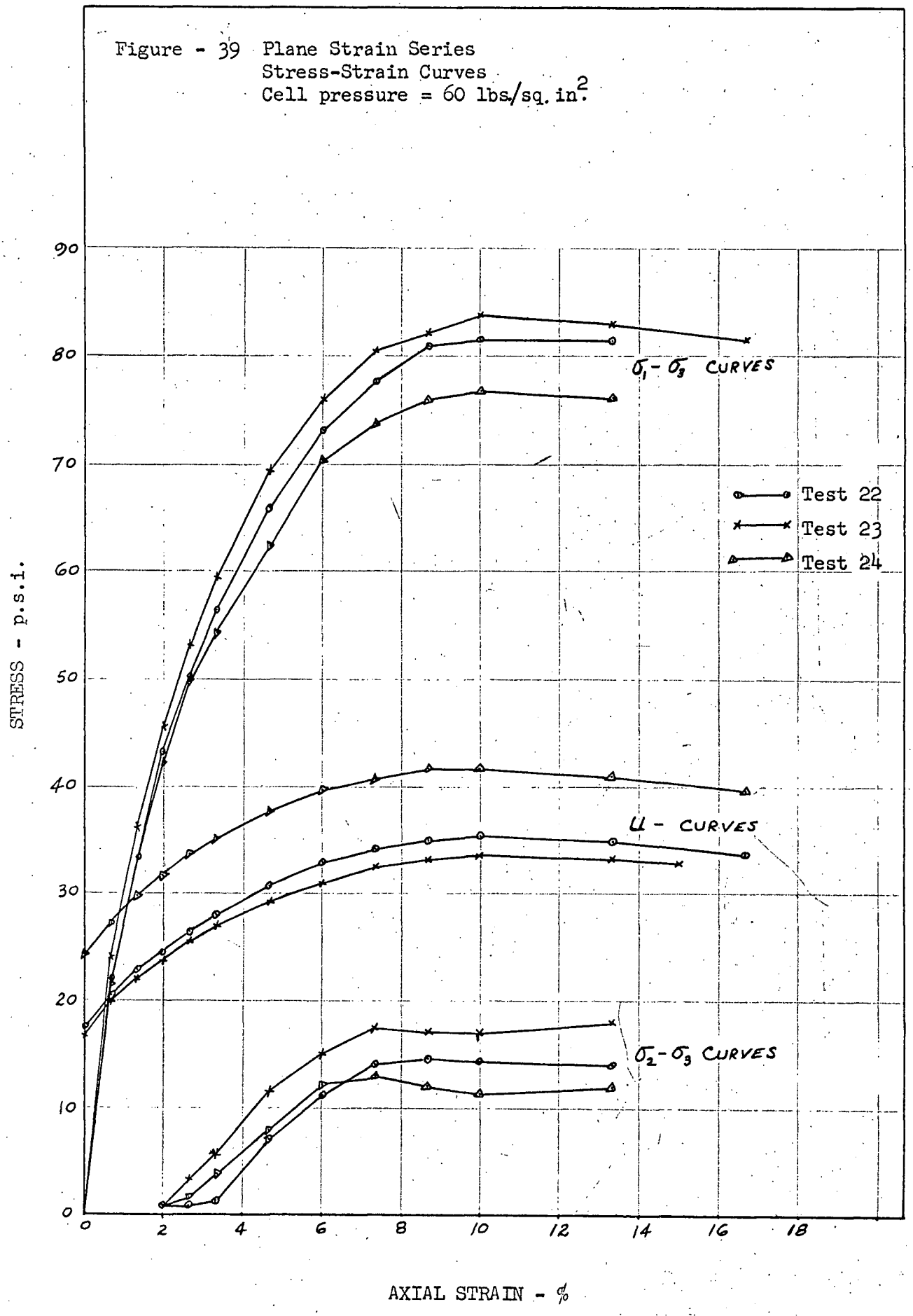

Figure - 40 Plane Strain Series
Stress-Strain Curves
Cell pressure = 75 lbs/sq. in.^{2}

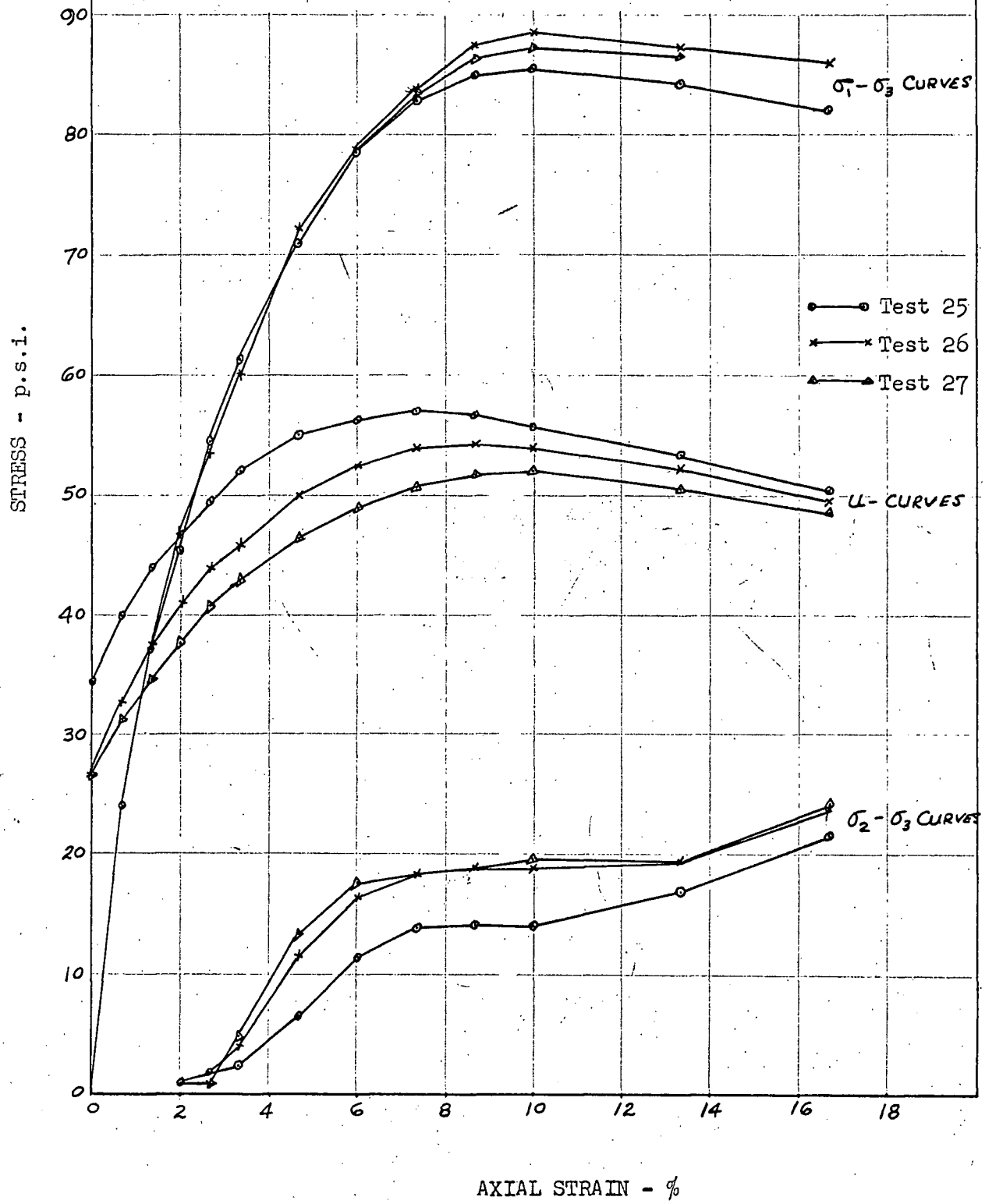

APPENDIX II

SAMPLE CALCULATIONS BASED ON DATA OBTAINED IN TEST NO. 19

A. Deviator Stress

(i) Corrected Area

$$a = \frac{ao}{1 - \epsilon}$$

$$= \frac{4.45}{1 - .0866} = 4.87 \text{ in.}^2$$

where

a = the area on which true deviator stress is calculated (in.^2)

ao = the initial area (in.^2)

ϵ = the axial strain ($^{\text{ins.}}/_{\text{in.}}$)

(ii) Vertical friction force because of plane strain plates.

$$F = \text{Average } (\sigma_2 - \sigma_3) \times 2 \times \text{Side Area} \times f$$

$$= 6.9\ (2)(3.82)(.05) = 2.6 \text{ lbs.}$$

where

F = friction force opposing the axial strain (lbs.)

f = co-efficient of friction of teflon

Then the deviator stress is calculated as follows:

$$\sigma_1 - \sigma_3 = \frac{286.5 - 2.6}{4.87} = 58.3 \text{ psi}$$

B. Secant Modulus of Deformation (M_{50})

$$M_{50} = \frac{\text{Max } (\sigma_1 - \sigma_3)(\text{psi})}{\text{axial strain } (\frac{\text{ins.}}{\text{in.}})}$$

$$= \frac{29.1}{.0133} = 2190 \text{ lbs/in.}^2$$

C. Pore Pressure Parameters

(i) Parameter B

$$B = \frac{Uo}{3} = \frac{18.7}{30} = .625$$

where

Uo = pore pressure change during the application of cell pressure, assuming that the pore pressure is equal to zero before the start of the test. (lbs/in.^{2}).

(ii) Parameter A_f

$$A_f = \frac{\Delta U}{\sigma_1 - \sigma_3} = \frac{6.2}{58.3} = 0.106$$

where

$\Delta U = U - Uo$

U = pore pressure at failure (lbs/in.^{2})

D. Vector Curves

The most convenient method of plotting the Vector curves is to calculate the co-ordinates of individual points analytically, using the following equations:

$$\bar{\sigma}_f = \bar{\sigma}_3 + (\sigma_1 - \sigma_3) \cos^2 \alpha_f$$

$$\tau_f = (\sigma_1 - \sigma_3) \sin \alpha_f \cos \alpha_f$$

where

$\alpha_f = 45^\circ + \frac{\phi'}{2}$, the angle between failure plane and major principal plane.

$\bar{\sigma}_f$ = effective normal stress on failure plane.

τ_f = shear stress on failure plane

and ϕ' = internal friction angle.

$$\bar{\sigma}_f(60^\circ) = 5.0 + 58.3 \left(\frac{1}{4}\right)$$

$$= 19.6 \text{ (lbs/in.}^2\text{)}$$

$$\tau_f(60^\circ) = 58.3 \left(\frac{3}{2}\right)\left(\frac{1}{2}\right)$$

$$= 25.3 \text{ (lbs/in.}^2\text{)}$$

REFERENCES

1. Bishop, A.W. (1955), Lecture delivered in Oslo, entitled "The Principle of Effective Stress". Printed in Tek. Ukeblad, No. 39 (1959) (Norwegian Geotechnical Institute. Publ., 32.)

2. Bishop, A.W., Alpan, J. Blight, G. and Donald, V. (1960), "Factors Controlling the Strength of Partly Saturated Soils." Research Conference on Shear Strength of Cohesive Soils Proceedings.

3. Bishop, A.W., and Bjerrum, L. (1960), "The Relevance of the Triaxial Test to the Solution of Stability Problems." Research Conference on Shear Strength of Cohesive Soils. Proceedings.

4. Bishop, A.W., and Henkel, D.G. (1957), "The Measurement of Soil Properties in the Triaxial Test". London, Arnold.

5. Casagrande, A., and Hirschfeld, R.C. (1960), "First Progress Report on Investigation of Stress Deformation and Strength Characteristics of Clays". (Report to Waterways Experiment Station.) Soil Mechanics Series No. 61, Harvard University, Cambridge, Massachusetts.

6. Gibbs, H.J., Hilf, J.W., Holtz, W.G. and Walker, F.C. (1960), "Shear Strength of Cohesive Soils." Research Conference on Shear Strength of Cohesive Soils. Proceedings.

7. Henkel, D.J. (1960), "The Shear Strength of Saturated Remoulded Clays." Research Conference on Shear Strength of Cohesive Soils. Proceedings.

8. Hilf, J.W. (1956), "An Investigation of Pore Water Pressure in Compacted Cohesive Soils". (Doctoral Thesis, University of Colorado), U.S. Department of the Interior, Bureau of Reclamation, Technical Memorandum 654, Denver, Colorado.

9. Lambe, T.W. (1951), "Soil Testing for Engineers". New York: John Wiley.

10. Leonards, G.A. ( ), "Foundation Engineering." McGraw Hill and Company.

11. Seed, H.B., Mitchell, J.K., and Chan, C.K. (1960), "The Strength of Compacted Cohesive Soils." Research Conference on Shear Strength of Cohesive Soils. Proceedings.

12. Skempton, A.W. (1954), "The Pore Pressure Co-efficients A and B." Geotechnique, Vol. 4, No. 4, pp 143 - 147.

13. Skempton, A.W. (1960), "Effective Stress in Soils, Concrete, and Rock". Conference on Pore Pressure and Suction in Soils. Butterworth, London.

14. Taylor, D.W. (1948), "Fundamentals of Soil Mechanics". New York: John Wiley.

15. Terzaghi, K. (1923), "Die Berechnung der Durchlassigkeitsziffer des Tones aus dem Verlauf der Hydrodynamischen Spannungserscheinungen." Sitz, Akad. Wissen. Wien Math-natunv. Kl. Abt. 11a, 132, 125 - 138.

16. Wilson, S.D. (1950), "Small Soil Compaction Apparatus Duplicates Field Results Closely". Engineering News Record, November, 1950.